



Cite this: *Nanoscale*, 2024, **16**, 14168

# Transforming textile waste into nanocellulose for a circular future†

Thenapakiam Sathasivam,<sup>a</sup> Sigit Sugiarto,<sup>a</sup> Michelle Pek Yin Yew,<sup>b</sup> Xin Yi Oh,<sup>a</sup> Siew Yin Chan,<sup>b</sup> Benjamin Qi Yu Chan,<sup>b</sup> Mao Jie Tim<sup>c</sup> and Dan Kai<sup>b</sup> \*<sup>a,b,d</sup>

The expansion of the textile industry and improvements in living standards have led to increased cotton textile production, resulting in a rise in textile waste, with cotton accounting for 24% of total textile waste. Effective waste management through recycling and reuse is crucial to reducing global waste production. Nanocellulose has diverse applications in environmental, geotechnical, food packaging, and biomedical engineering areas. As interest in nanocellulose's unique properties grows, cotton-based textile waste emerges as a promising source for nanocellulose development. However, there is a notable lack of comprehensive reviews on the extraction of nanocellulose from textile waste as a sustainable biomaterial. This paper aims to address this gap by exploring current extraction processes, properties, and recent applications of nanocellulose derived from textile waste. We discussed (1) the potential of nanocellulose resources from different textile wastes, (2) a comparison of the various extraction methods, (3) the functionalization technology and the potential application of such nanocellulose in the textile industry, and (4) the life cycle assessment (LCA) and potential gap of the current technology. It also emphasizes the potential reintegration of extracted nanocellulose into the textile industry to manufacture high-value products, thus completing the loop and strengthening the circular economy.

Received 29th April 2024,  
Accepted 2nd July 2024

DOI: 10.1039/d4nr01839g

[rsc.li/nanoscale](https://rsc.li/nanoscale)

## 1. Introduction

The textile industry plays a vital role in our lives, but its production, usage, and disposal have significant environmental implications.<sup>1</sup> The rise of fast fashion, characterized by low-cost manufacturing, frequent consumption, and short garment lifespans, has contributed to a substantial increase in clothing waste generation, resulting in economic, environmental, and social challenges.<sup>2,3</sup> Incineration and landfilling are widely adopted techniques for managing textile waste globally, primarily due to their cost-effective disposal methods. However, significant quantities of greenhouse gases, toxic chemicals, and unpleasant odors are emitted into the environment due to the anaerobic decomposition of cellulose in land-

fill sites and the combustion of cellulose in incinerators. This leads to pollution of the air, land, and water in the surrounding areas.<sup>4</sup> As the textile industry navigates a critical juncture, it confronts an unprecedented mandate for sustainability to address escalating environmental crises and shifting consumer trends. While prioritizing reuse as the preferred method for managing end-of-life textiles, the advancement of recycling technologies becomes crucial in addressing non-rewearable, worn-out, and damaged textiles unsuitable for reuse.<sup>5,6</sup>

Cellulose, the source of nanocellulose, is a polysaccharide composed of glucose monomers linked through  $\beta$ -1,4-glycosidic bonds, exhibiting hydrophilic hydroxyl groups and hydrophobic axial carbon-hydrogen (C-H) planes.<sup>7,8</sup> Its dense packing and amphiphilic nature stem from intra- and intermolecular hydrogen bonds, leading to highly ordered crystalline structures.<sup>9</sup> The size of nanocellulose fibers typically measures less than 100 nanometers in diameter and several micrometers in length. Nanocellulose from cotton-based textile waste could be classified as two main types which are cellulose nanocrystal (CNC) and cellulose nanofibril (CNF). Even though these types share a similar chemical composition, they differ in morphology, particle size, crystallinity, and other properties due to variations in the sources and extraction methods.<sup>10</sup> CNC, also known as cellulose nanocrystals or cellulose nanowhiskers, is a type of nanocellulose with high strength and is typically obtained from cellulose fibrils

<sup>a</sup>Institute of Sustainability for Chemicals, Energy and Environment (ISCE2), The Agency for Science, Technology and Research (A\*STAR), 2 Fusionopolis Way, Innovis, #08-03, 138634 Singapore, Singapore. E-mail: [kaid@imre.a-star.edu.sg](mailto:kaid@imre.a-star.edu.sg)

<sup>b</sup>Institute of Materials Research and Engineering (IMRE), The Agency for Science, Technology and Research (A\*STAR), 2 Fusionopolis Way, Innovis, #08-03, 138634 Singapore, Singapore

<sup>c</sup>Chemical & Biomolecular Engineering, College of Design and Engineering, National University of Singapore, 4 Engineering Drive 4, Singapore 117585, Singapore

<sup>d</sup>School of Chemistry, Chemical Engineering and Biotechnology, Nanyang Technological University, 21 Nanyang Link, Singapore 637371, Singapore

† Electronic supplementary information (ESI) available. See DOI: <https://doi.org/10.1039/d4nr01839g>



through acid hydrolysis. It exhibits a short-rod-like or whisker shape, with diameters ranging from 2 to 20 nanometers and lengths between 100 and 500 nm.<sup>10</sup> CNF, also referred to as cellulose nanofibers or cellulose nanofibrils, is a form of nanocellulose characterized by its long, flexible, and intertwined structure, and is extracted from cellulose fibrils through mechanical means. It adopts elongated fibril shapes with diameters ranging from 1 to 100 nm and lengths spanning from 500 to 2000 nm.

In recent studies, there has been a surge in interest towards utilizing cotton-based textiles, which constitute a significant portion of fabric waste, and are emerging as an especially promising source for the extraction of nanocellulose. Cotton-based textile waste presents a potential source of nanocellulose given that cotton fibers consist of about 94% cellulose by weight that would possess exceptional properties suitable for various high-value applications.<sup>11</sup> Extracting nanocellulose from textile materials holds immense promise in nanotechnology.

Nanocellulose is utilized across various applications and exhibits a myriad of strengths including impressive mechanical robustness, flexibility, optical transparency, and a high surface area volume ratio.<sup>11</sup> These characteristics render nanocellulose an invaluable resource for enhancing the functional properties of textiles, such as improving tensile strength, enhancing moisture management, and enabling the incorporation of novel functionalities. nanocellulose derived from cotton textile waste offers a promising avenue for advancing

low-carbon and circular development. By extracting nanocellulose from cotton textile waste, we can effectively repurpose this material, reducing the need for virgin resources and mitigating waste disposal issues. This approach aligns with circular economy principles by extending the lifespan of cotton fibers and minimizing the environmental impact. By repurposing textile waste into nanocellulose for various applications (Fig. 1), the environmental impact of textile disposal may be mitigated while promoting the sustainable production of advanced materials.

This comprehensive review aims to provide an in-depth exploration of examining, sorting, pre-treatment, and isolation methods for extracting nanocellulose from textile waste. Our discussion will include various ways involving nanocellulose extraction, comprising mechanical disintegration, chemical processing, and enzymatic methods. We aim to highlight the merits and demerits along with recent innovations associated with each technique. We also intend to explore nanocellulose's potential in textile industry applications. A crucial aspect this review will concentrate on the combination of nanocellulose with other nanomaterials like nanoparticles, nanoclays, and carbon nanotubes, aiming at devising advanced hybrid materials that enhance the performance characteristics for specific applications. Furthermore, we aim to delve into the nascent domain of smart-functional textiles where nanocellulose plays a key role empowering the creation of wearable electronic devices, responsive fabrics and biodegradable sensors.

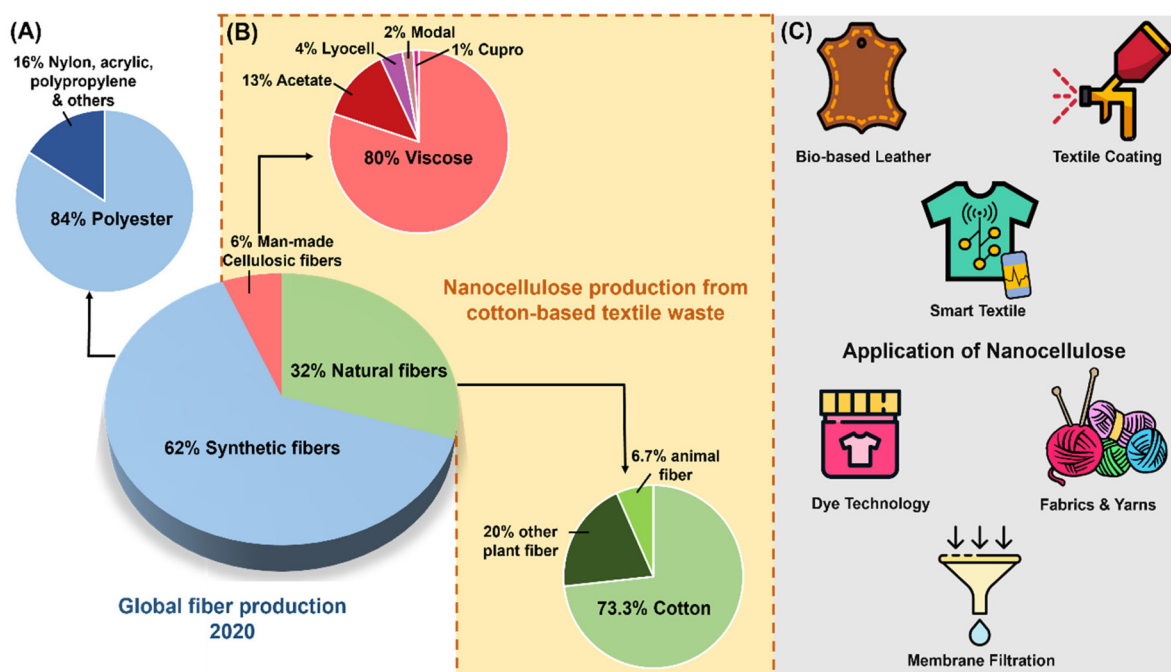


**Fig. 1** (A) World production of fibres estimated for the year 2021, comprising synthetic (blue), natural (green) and man-made cellulosic (red) fibres. Different fibre types in specific fibre groups and their production volume in percentages are shown separately in blue, red, or green in the pie chart. Adapted figures were produced using data from the Preferred Fiber and Materials Market Report 2022 of the Textile Exchange Organization.<sup>12</sup> (B) Nanocellulose extracted from cotton-based textile waste. (C) Application of nanocellulose in the textile industry.



## 2. Types of cotton used in the textile industry

Cotton holds the second position, accounting for 23% of total fiber usage, while polyester (PET), a synthetic fiber, leads the global fiber manufacturing market with a market share of approximately 52%.<sup>13</sup> This disparity in cellulose availability presents opportunities for the development of man-made cellulosic fibers (MMCF). MMCFs are regenerated cellulosic fibers (RCF) derived from cellulose extracted from wood pulp, which is subsequently chemically dissolved and extruded into staple fibers. Viscose, acetate, cuprammonium, and Lyocell methods are among the various types of man-made cellulosic fiber available.

### 2.1 Viscose rayon

The Viscose process is widely used to create regenerative cellulosic fibers (RCF) and is typically sourced from wood pulp obtained from rapidly growing trees like bamboo, pine, sugar cane, beech, and eucalyptus. Fig. 2A illustrates the schematic of the Viscose process. This method involves immersing the pulp in sodium hydroxide for a specific period, and then shredding and aging it as shown in Fig. 3A. The pulp's viscosity is affected by the duration of aging. Following this, the pulp is mixed with carbon disulfide (CS<sub>2</sub>) to form cellulose xanthate, which is then dissolved in sodium hydroxide to initiate the Viscose fiber formation process.<sup>14</sup> The dissolved pulp is precipitated in acid using wet-spinning equipment to neutralize and regenerate cellulose simultaneously. Subsequent washing steps are used to produce pure cellulose regenerated fiber.<sup>15</sup> Currently, about 70% of

carbon disulfide can be recycled, while the remainder is converted into sulfuric acid (H<sub>2</sub>SO<sub>4</sub>) and also recovered.<sup>16</sup> However, the Viscose process has environmental concerns due to the high chemical usage (e.g. NaOH), leading to the production of sodium sulfate as a by-product.

### 2.2 Lyocell rayon

Lyocell is notable for its closed-loop system of production, wherein non-derivative solvents like *N*-methylmorpholine-*N*-oxide (NMMO) are utilized to dissolve cellulose and are then recycled and repurposed (Fig. 2B). This approach has the potential to streamline the production of RCF by eliminating multiple steps (Fig. 3B).<sup>21</sup> This technology involves direct cellulose dissolution, making it a simpler process with reduced chemical usage compared with the traditional Viscose method. Furthermore, direct solvents are simpler to recycle as they do not produce any byproducts, contributing to a more environmentally sustainable method.<sup>21</sup> Lyocell fibers demonstrate superior characteristics such as higher tenacity (especially in wet conditions), increased modulus, reduced shrinkage, improved thermal stability, higher crystallinity, and greater orientation when compared with Viscose.<sup>22</sup> However, the manufacturing expenses associated with Lyocell exceed those of Viscose because of the utilization of costly solvents and the necessity for high temperatures to dissolve cellulose.<sup>23</sup>

### 2.3 Cellulose acetate

While less frequently utilized, another method for fiber production involves acquiring cellulose acetate. Cellulose acetate

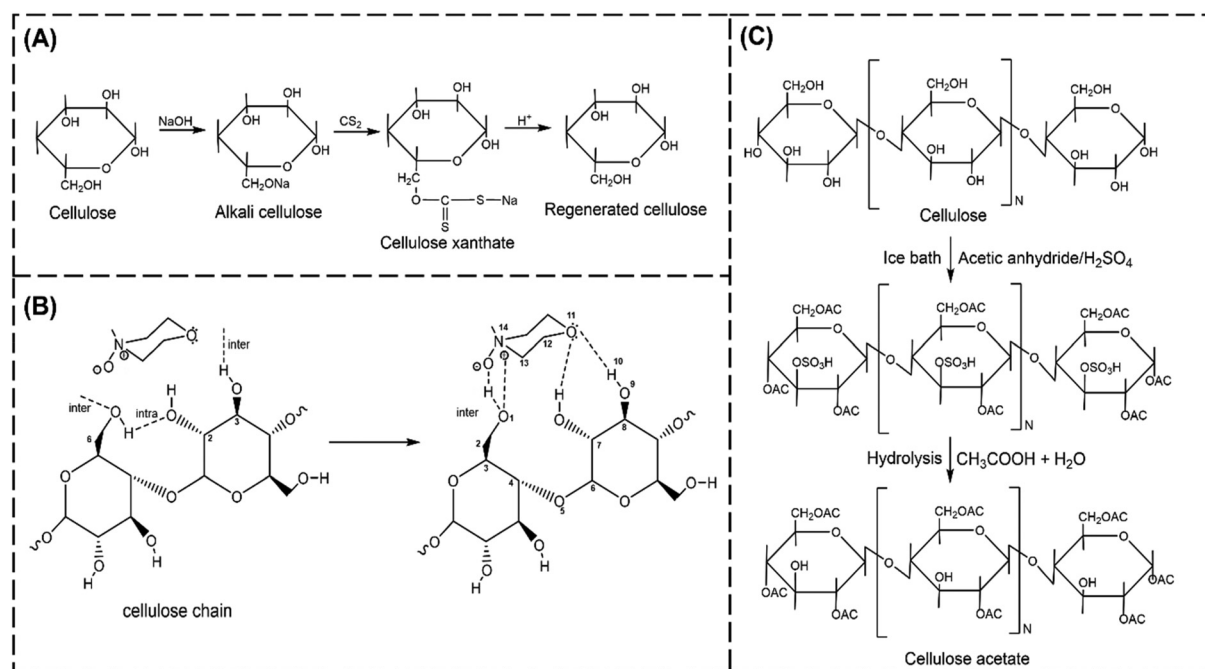


**Fig. 2** Mechanism of processes involved in the textile industry. (A) Viscose fiber production, adapted from ref. 17 and 18. Copyright (2013) and (2017) ScienceDirect, (B) NMMO–cellulose dissolution in the Lyocell process, reprinted with permission from ref. 19. Copyright (2010) American Chemical Society, and (C) cellulose acetate preparation (adapted from ref. 20). Copyright (2019) Springer.



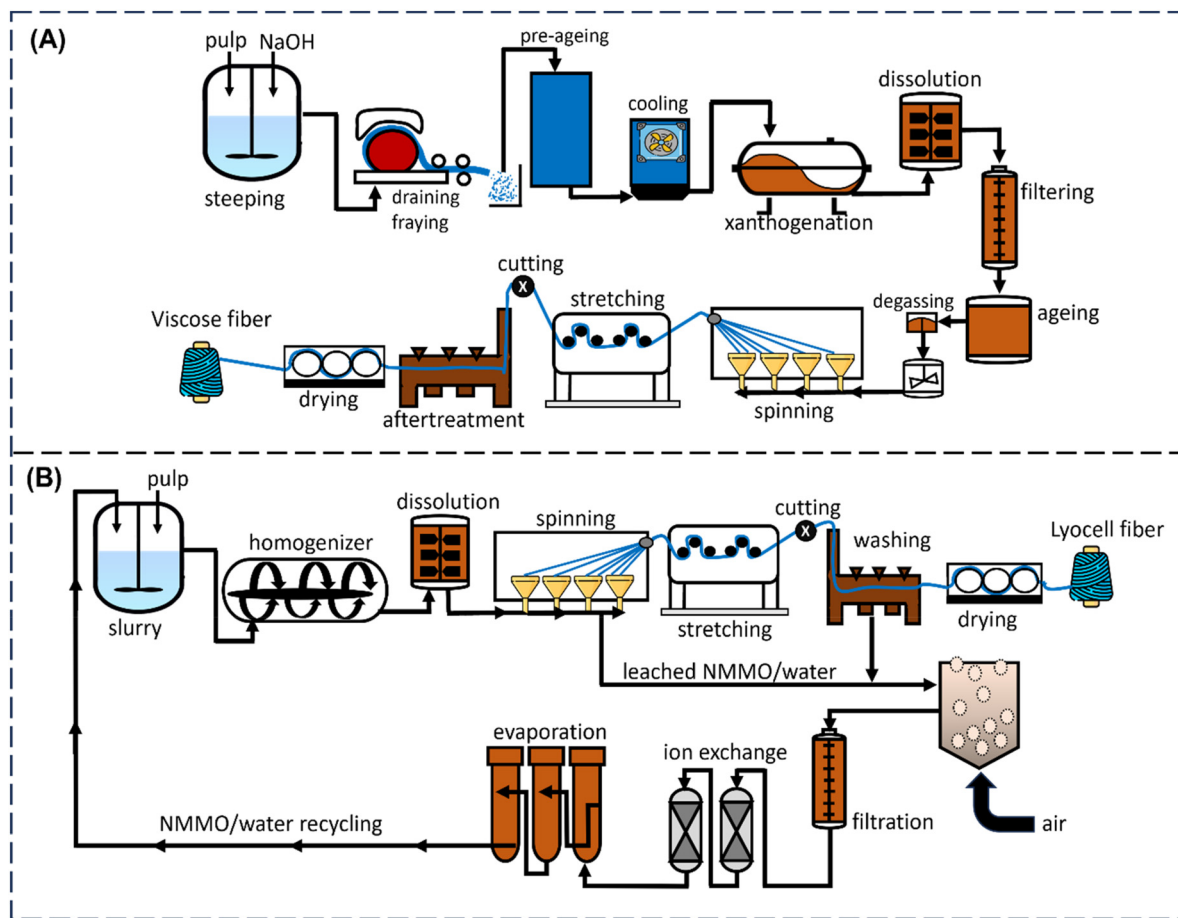


Fig. 3 Schematics of fiber production. (A) Viscose process and (B) Lyocell process (adapted from ref. 20). Copyright (2019) Springer.

is produced through a process where cellulose pulp reacts with acetic anhydride to form acetate flakes (Fig. 2C). Subsequently, these flakes are dissolved in a solvent to form a cellulose solution.<sup>24</sup> Cellulose dissolves in a solution containing acetic acid and acetic anhydride, with the process occurring in the presence of a catalyst, such as sulfuric acid.

Controlled partial hydrolysis of cellulose acetate is subsequently carried out to eliminate sulfate and several acetate groups, resulting in the desired product properties. The cellulose solution is subsequently passed through a spinneret, where yarns are formed by evaporating the solvent. This technique is known as the dry-spinning method.<sup>20</sup> However, cellulose acetate fibers are not widely used in the textile industry due to their low strength, poor abrasion resistance, and thermal retention.<sup>25</sup>

#### 2.4 Cuprammonium rayon

Cuprammonium rayon, also referred to as cupro, is typically obtained from cotton linters, a residual material from the cotton plant. The linters are dissolved into a cuprammonium solution, which is a mixture of copper and ammonium.<sup>26</sup> These were then dropped into caustic soda and extruded through a spinneret, resulting in the production of cupro fibers. Cupro, while not as robust as some other rayon varieties,

is still recognized for its durability.<sup>27</sup> It surpasses viscose and silk in strength, making it a preferable choice for those seeking a resilient and sophisticated alternative to silk, especially considering the high cost of silk. Cupro is typically considered less sustainable due to its chemical-intensive manufacturing process. While some chemical solutions can be recycled, the final disposal is toxic and necessitates stringent control measures.<sup>20</sup>

#### 2.5 Blends with other polymer fibers

In the textile market, composite fabrics comprising cellulose and other fibers like PET, silk, wool, viscose, polyamide, or polyurethane are widely established. These blends are spun together in a spinning process to improve moisture absorbency, strength, shape retention and texture compared with individual fabrics. For instance, PET fabric is naturally hydrophobic and more electrostatic compared with natural fibers.<sup>28</sup> Conversely, cotton fabric, being hydrophilic, has better moisture absorption but demonstrates poor wicking properties between the inner and outer surfaces of the fabric, which may not be suitable for wear during energetic activity.<sup>29</sup> Therefore, polyester/cotton blends are employed to counteract these limitations, providing improved moisture management and wicking capabilities.<sup>30</sup> Similarly, silk/cotton blends have been





investigated using Eri silk.<sup>31</sup> Their findings suggest that an increase in silk fiber content in the yarn enhances tensile strength and breaking elongation values. However, these wastes are heterogeneous and comprise a blend of natural and synthetic fiber materials, which complicates both fiber recovery and disposal.<sup>32</sup> The recycling methods for these blends can be generally classified into two categories, depending on whether the two mixed components are separated or not.

### 3. Extraction of nanocellulose from cotton-based textile waste

#### 3.1 Physical and mechanical treatment

Physical treatment methods such as steam or autohydrolysis, hydrothermolysis, aquasolv, uncatalyzed solvolysis, and wet oxidation, are utilized to break down textile waste into finer particles.<sup>33,34</sup> Physical treatment involves subjecting the textile waste to high pressure and temperature to eliminate impurities while keeping the water in a liquid state during hydrothermolysis.<sup>35</sup> This process typically occurs at temperatures ranging from 200 to 230 °C and lasts for a few minutes. Approximately 60% of the textile material is dissolved into small particles dispersed in water during this phase. The objective of physical treatment is to convert the textile waste into tiny fiber forms and eliminate dirt. However, since lignocellulose particles break apart during chemical treatment, neither physical nor mechanical treatment results in a significant reduction in the amount of textile waste. Pérez *et al.* investigated the effects of the temperature (170 and 200 °C), solid content (5% and 10% w/v), residence duration (0 and 40 min), and reactor overpressure (30 bar) of physical pretreatment on the enzymatic hydrolysis process.<sup>36</sup> They evaluated pretreatment efficiency by comparing the solid composition obtained from pretreatment with that of solid samples without pretreatment. Studies have shown that pretreatment influences temperature and residence time, with increased time and temperature enhancing enzyme hydrolysis yields.<sup>37</sup> Various physical treatment studies have been conducted to optimize these processes by adjusting the treatment time, strain, and temperature.<sup>38</sup> It is crucial to select the appropriate treatment system to monitor the decomposition route of substances by varying parameters such as the temperature, pressure, and duration of the hydrothermolysis treatment.<sup>39</sup>

The mechanical treatment of textile waste is widely utilized due to its simplicity and cost-effectiveness compared with alternative methods. This process involves the mechanical processing and shredding of textile waste, and it is applicable to various fibers like PET, cotton, *etc.* However, the shredding method frequently results in a reduced fiber length from textile waste, directly affecting the original fiber quality and mechanical properties. These fibers are typically blended with virgin fibers in specific proportions to enhance the overall quality.<sup>40</sup> Mechanical treatment complicates the reproduction of yarns or nanocellulose from the derived fibers. The mechanical forces exerted during shredding, as well as the aging of

fibers and the abrasion caused by detergent during washing, decrease the degree of polymerization (DP) in cellulose. This decreased DP adversely affects fiber length and strength, posing challenges in the quality of nanocellulose or yarn production.<sup>41</sup> In a particular study, researchers highlighted that the primary concern is the initial yarn production rather than the level of wear in mechanically shredded textile waste.<sup>42</sup> Considering that the fibers obtained are shortened, it is advisable to avoid ring spinning and instead opt for rotor or friction spinning. Wet mechanical equipment has been employed to separate cotton from synthetic fibers in denim fabric. This separated material can then be reused to create RCF and yarns for textile production. The system utilized laboratory screens and hydrocyclones, although some operational issues were encountered with this method.<sup>43</sup>

In an alternative investigation, a brief static acid treatment lasting one minute was applied to mixed cellulose and polyester fabrics.<sup>44</sup> This treatment involved immersing the fabrics in a 95 °C aqueous sulphuric acid (H<sub>2</sub>SO<sub>4</sub>) solution before subjecting them to mechanical beating (stirring) in water at room temperature. This procedure led to the removal of cellulose from the blended fabrics in the form of a powder, while the polyester was reclaimed for subsequent use in new fabric production. The fibers obtained from this process were transformed into nonwoven webs designed for insulation purposes.<sup>45</sup> For instance, a denim fabric made from a blend of cotton and polyester underwent treatment with a 10 wt% H<sub>2</sub>SO<sub>4</sub> solution and was heated to 90 °C. Subsequently, the mechanical fractionation process was carried out, and the fibers were sifted through a mesh to separate the two components. Following these steps resulted in obtaining both polyester fibers and cotton fiber powder. The recuperated cotton was utilized for extracting cellulose nanocrystals intended for incorporation into composites.<sup>46</sup> Ball milling is another method used to produce nanocellulose, which can be carried out in either dry or wet conditions. In dry ball milling, the cellulose undergoes decrystallization, while wet ball milling involves the addition of liquid to prevent or slow down the decrystallization. Kang *et al.* employed wet ball milling followed by centrifugation, an environmentally friendly approach, to create cellulose nanocrystals (CNCs) from three distinct cellulosic sources: microcrystalline cellulose (MCC), bleached Kraft pulp, and CF11 cellulose.<sup>47</sup> Varying the ball milling time from 0.6 to 16 hours, they observed a rapid increase in nanocrystal yield from MCC and CF11 cellulose within the first 4 hours, followed by a nearly constant yield after 8 hours. Because no chemical agents are used in this synthesis, both the crystallinity and thermal stability of the raw cellulose and the synthesized CNCs were discovered to be almost comparable. Fig. 4 shows the various types of nanocellulose synthesis from textile waste.

#### 3.2 Chemical treatment

**3.2.1 Hydrolysis.** Acid hydrolysis is a well-established chemical technique utilized for extracting nanocellulose from cellulosic fibers. This process commonly employs potent



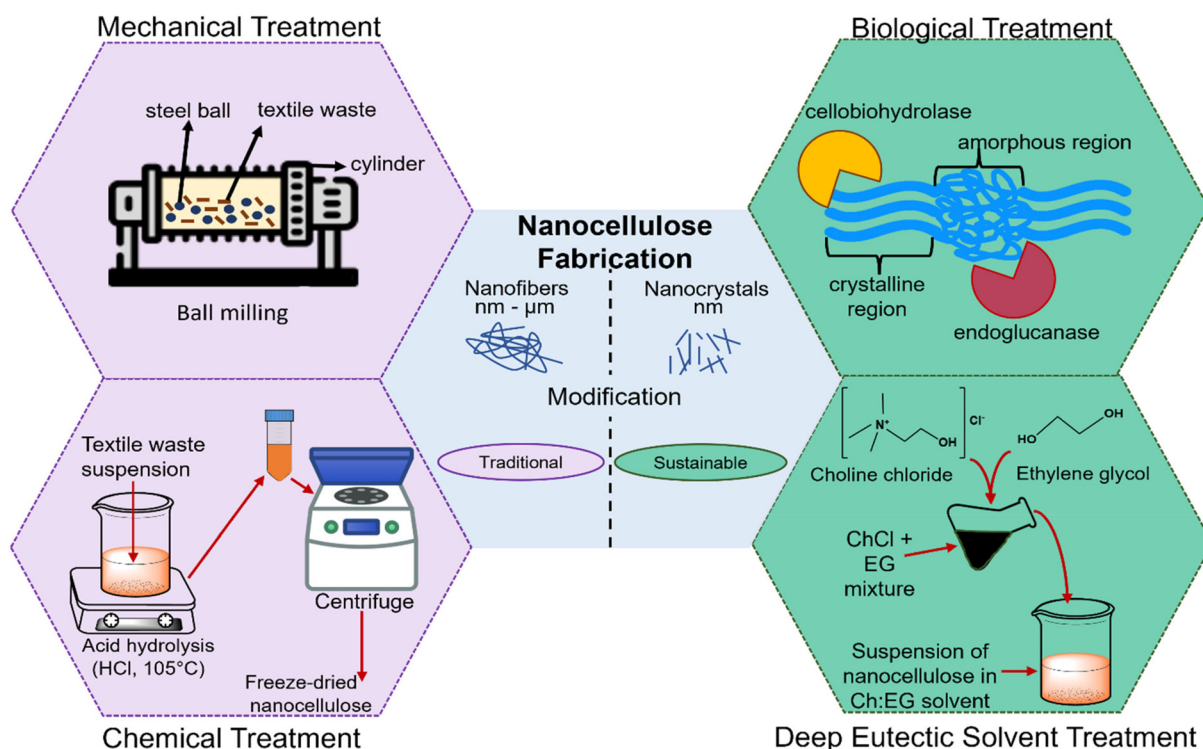


Fig. 4 The various types of nanocellulose synthesis.

mineral acids, like  $\text{H}_2\text{SO}_4$  or hydrochloric acid (HCl). The hydrolysis reaction involves the depolymerization of cellulose, where hydronium ions ( $\text{H}^+$ ) infiltrate the amorphous segments of the cellulose chains, inducing a hydrolytic cleavage of glycosidic bonds.<sup>48</sup> This results in the breakdown of cellulosic fibers into nanocellulose. Unlike synthetic polymers, this nanocellulose cannot be reconstituted into larger cellulosic polymeric chains.

Sulfuric acid is the most frequently used hydrolysing agent due to its ability to initiate the esterification in cellulose involving the hydroxyl groups through anionic sulfate ions.<sup>49</sup> Moreover, the presence of anionic groups contributes to the formation of a negative electrostatic layer on the surface of the nanocellulose, facilitating their dispersion in water and leading to the formation of stable colloid systems.<sup>10</sup> Other acids, including hydrobromic acid (HBr), nitric acid ( $\text{HNO}_3$ ), and phosphoric acid ( $\text{H}_3\text{PO}_4$ ), have also shown successful application in acid hydrolysis. For instance, Zhong *et al.* successfully isolated nanocellulose from indigo-dyed denim fabric and bleached cotton using acid hydrolysis combined with high-intensity ultrasonication (HIUS). The resulting nanocellulose from indigo-dyed denim had a width of  $12.5 \pm 4.3$  nm, length of  $151.7 \pm 52.6$  nm, crystallinity of 85.6%, and yield of 37.8%. For the nanocellulose obtained from bleached cotton, the width ranged over  $11.9 \pm 6.7$  nm, length ranged over  $127.7 \pm 43.8$  nm, crystallinity was 86.4%, and the yield reached 39.6%.<sup>50</sup> These findings highlight the effectiveness of acid hydrolysis allied with HIUS in producing nanocellulose from

different cellulose sources. Furthermore, Pandi *et al.* successfully isolated nanocellulose from cotton waste using HIUS paired with sulfuric acid hydrolysis. They reported the nanocellulose isolated had a fiber diameter ranging over 10–50 nm and a crystallinity index of 81.23%.<sup>51</sup> Cao *et al.* produced a CNC suspension by subjecting waste cotton fabric to  $\text{H}_2\text{SO}_4$  treatment and generated a transparent composite film of CNCs and cellulose acetate which has potential applications in disposable packaging materials, sheet coating and binder products.<sup>52</sup>

The presence of non-crystalline hemicellulose and lignin components in cotton fibers typically diminishes both the crystalline nature and mechanical strength of the resulting CNCs. As suggested by Morais *et al.* it is advisable to eliminate these non-crystalline constituents through a straightforward alkaline hydrolysis process.<sup>53</sup> Thambiraj and Shankaran outlined a CNC production method involving waste cotton, which entailed a series of steps including alkali pre-treatment followed by  $\text{H}_2\text{SO}_4$  treatment.<sup>54</sup> In this process,  $\text{H}_2\text{SO}_4$  hydrolysis effectively removed hemicellulose, lignin, and other impurities, resulting in the production of micrometer-sized needle-like CNCs which exhibit mechanical properties that are comparable to steel and aluminum, as demonstrated by Kuo *et al.*<sup>55</sup> Notably, the aspect ratio of the needle-like CNCs produced *via* the combined alkali and acid hydrolysis (ranging from 14 to 40) surpassed that of CNCs obtained through acid hydrolysis alone (with aspect ratios of 10 to 20), indicating an enhancement in mechanical performance.



**3.2.2 TEMPO (2,2,6,6-tetramethylpiperidine 1-oxyl) mediated oxidation.** TEMPO oxidation is another chemical method for producing nanocellulose from cellulosic fibers. TEMPO oxidation is commonly used in conjunction with a mechanical method to disaggregate the cellulose fibers. The main goal of utilizing TEMPO is to reduce the energy required for mechanical disintegration by diminishing the negative or positive charge on the surfaces of the fibres and by improving the colloidal suspension's stability of the produced nanocellulose. TEMPO-mediated oxidation treatment is generally carried out in the presence of bleaching agents such as NaClO and catalysts such as sodium bromide (NaBr) under alkaline conditions. Despite lowering the energy consumption, this method has several disadvantages, such as toxic reagents, low efficiency and an inability to recover the chemicals.<sup>56</sup> Zhong *et al.* utilised TEMPO/NaBr/NaClO at pH 10–10.5 on indigo-dyed denim and bleached cotton followed by centrifugation, dialysis and microfluidization. They reported obtaining nanocellulose with a width between  $9.90 \pm 3.8$  nm, length of  $162.3 \pm 86$  nm, crystallinity index of 66.0% and yield of 78.9% from indigo-dyed denim and nanocellulose with a width of  $11.4 \pm 5.3$  nm, length of  $175.2 \pm 93.0$  nm, crystallinity index of 71.6% and yield of 72.6%.<sup>50</sup>

**3.2.3 Ammonium persulfate oxidation (APS).** APS emerges as an alternative chemical method to produce nanocellulose. APS exhibits favourable characteristics, including high solubility in water and low toxicity, making it a suitable candidate for generating  $\text{H}_2\text{O}_2$  and  $\text{SO}_4^{2-}$  free radicals under acidic conditions and elevated temperatures. These radicals play a crucial role in solubilizing the amorphous cellulose fraction as well as lignin content.<sup>57</sup> In a study conducted by Ye *et al.*, nanocellulose was extracted from viscose fiber waste using the APS oxidation method. It is reported that the size of nanocellulose reduces with increased reaction time, higher temperature and increased APS concentration.<sup>58</sup> More recently, Culsum *et al.* employed the APS oxidation method to extract nanocellulose from denim waste. They reported that under optimum conditions (15 h, 60 °C and 1.5 M APS), the produced nanocellulose had diameters of  $18.10 \pm 3.54$  nm, was  $76.14 \pm 8.56$  nm in length, and had crystallinity of 83%.<sup>59</sup>

**3.2.4 Ionic liquid.** Cellulose presents challenges in terms of dissolution, necessitating the use of ionic liquids. However, these solvents tend to be costly and can escalate the overall process expenses unless they are reclaimed or recycled. Ionic liquids are a class of salts characterized by their liquid state at relatively low temperatures, typically below 100 °C. These compounds consist of large organic cations paired with small inorganic or organic anions. The unique properties of ionic liquids enable them to establish hydrogen bonds with the hydroxyl groups of cellulose, leading to the disruption of intermolecular hydrogen bonds within the cellulose structure and subsequent dissolution of cellulose. Their popularity stems from their capacity to dissolve cellulose while initiating minimal degradation of the molecular chains. The solubility of cellulose in ionic liquids is influenced by the length of the alkyl chain. Conversely, it is important to note that the solubi-

lity of cellulose from cotton does not consistently reduce as the length of the alkyl chain increases.<sup>60</sup> The RCFs occurs upon the addition of an antisolvent, such as water or ethanol, which induces the precipitation of nanocellulose.<sup>61,62</sup>

One widely recognized solvent for cellulose is *N*-methylmorpholine-*N*-oxide (NMMO). Notably, NMMO is environmentally degradable<sup>63</sup> and can function effectively under what are considered “gentle conditions” within the industry, including ambient pressure and temperatures below 130 °C. Consequently, the resulting dissolved cellulose could be processed into what is termed “regenerated cellulose”, which can be further transformed into fibers like Lyocell and viscose, or even regenerated into nanocellulose. Jaihanipour *et al.* employed NMMO as a solvent to extract cellulose from a 50/50 polyester/cotton blend with an orange color.<sup>64</sup> It is worth noting that they also utilized this method to dissolve regenerated cellulose from a 40/60 polyester/viscose blend in blue. This extraction process was conducted at a temperature of 120 °C. To isolate the cellulose, water was introduced into the solvent. Following the separation process, the polyesters were purified and recovered as fibers. They successfully obtained as much as 95% of the precipitated cellulose, which was collected on a filter for later use. Haule *et al.* initially processed waste cotton fabric by washing and breaking it down into fiber pulp.<sup>65</sup> This pulp was subsequently dissolved, along with propyl gallate, in an NMMO solution to create a regenerated cellulose solution. This solution was then used in the wet spinning process to produce RCF and exhibited greater tensile strength. This enhanced strength could be attributed to the axial stretching of the fibers during wet spinning, leading to crystallization and the growth of crystal grains. Nonetheless, the drawbacks associated with dissolving cellulose using the NMMO solvent encompass a high cost, harsh dissolution conditions, poor thermal stability, and the challenging retrieval of the solvent.

There are other ionic liquids are utilized for this purpose, with some of the most employed ones including 1-allyl-3-methylimidazoliumchloride ([AMIM]Cl), 1-ethyl-3-ethylimidazolium chloride ([EMIM]Cl), 1-butyl-3-methyl-imidazolium chloride ([Bmim]Cl), 3,3-dimethylimidazolium sulfoxide ([([MIM]2SO)]Cl<sub>2</sub>), 1-(2-hydroxyethyl)-3-ethylimidazolium chloride, and various others. Lv and colleagues manufactured RCFs using a process involving dewaxing, dissolution, filtration, and solidification of waste cotton blended fabrics.<sup>66</sup> Following dewaxing pre-treatment, the waste cotton blended fabrics were dissolved in a liquid containing 1-allyl-3-methylimidazolium chloride ([AMIM]Cl). The undissolved fibers were subsequently filtered, resulting in a cellulose/[AMIM]Cl solution. Finally, this solution was poured into water, leading to the formation of solid RCFs. The key principle behind this process is that [AMIM]Cl is soluble in water, while cellulose is not, causing cellulose to solidify into RCFs upon contact with water.

**3.2.5 Deep eutectic solvent.** Deep eutectic solvents (DESs) represents another category of substances that have been actively investigated for their potential use in cellulose dissolution. These substances often exhibit similar properties to



ionic liquids but are considered more cost-effective and environmentally sustainable. A DES is produced by the combination of two or three components: a quaternary ammonium salt with either a hydrogen bond donor or a metal salt.

An example of a well-known DES is derived from choline chloride and urea in a 1:2 mole ratio, which remains in a liquid state even at a low temperature (12 °C). Other common mixtures would be zinc chloride with choline chloride, cobalt (II) chloride hexahydrate with choline chloride, and zinc chloride with urea. Despite their potential as cellulose solvents, DESs tend to exhibit lower cellulose solubility rates compared with other solvents.<sup>67</sup>

Chen *et al.* have proposed several strategies to enhance cellulose solubility in DESs, such as the incorporation of strong hydrogen acceptors like morpholine, HCOO<sup>-</sup>, Cl<sup>-</sup>, and imidazole.<sup>68</sup> An alternative approach involves the use of surfactants and ultrasonic irradiation to enhance cellulose solubility by improving the permeability of DESs. DESs have also been employed for dissolving, modifying, and plasticizing cellulose from materials like cotton textiles (non-blended) and other cellulosic sources.<sup>69,70</sup> Ling and co-workers have created CNCs from cotton fibers using DESs with different ratios of choline chloride/oxalic acid dihydrate.<sup>71</sup> It was found that the CNCs produced with milder treatment exhibited lower crystallinity and lamellar structures.

There have been methods using deep eutectic solvents (DES) to separate cotton–polyester blends, offering a promising solution for the efficient recovery and recycling of these textile materials. Liu *et al.* have introduced an environmentally friendly method for the degradation and separation of PET from cotton which is highly significant in utilizing waste polyester/cotton blends by using betaine-based deep eutectic solvents (DESs).<sup>72</sup> The results revealed the PET fibers were entirely degraded, yielding a purified monomer, bis(2-hydroxyethyl terephthalate) (BHET), with an 85% yield, which can be repolymerized to produce PET. Moreover, 95% of the cotton was successfully recycled while preserving its original structural integrity. Similarly, in another research study PET and cellulose were extracted from waste polyester–cotton blended fabrics using choline chloride (ChCl) and *p*-toluenesulfonic acid (TsOH) as the treatment solvent.<sup>73</sup> The results revealed impressive yields of 99.20% for recycled PET (R-PET), 69.46% for microcrystalline cellulose (MCC), and 38.91% for glucose. Notably, the properties of R-PET remained largely unaffected. MCC exhibited a crystallinity of 86.46%, making it a viable raw material for NCC production. Table 1 presents the current extraction methods for converting pure cotton and cotton blend textile waste into nanocellulose.

### 3.3 Biological treatment

In recent years, there has been a focus on applying this method to recycle blended textile waste, separating fibers based on their composition. Typically, a cocktail of enzymes is employed to facilitate the isolation of nanocellulose from pre-treated cellulosic fibers. This enzymatic cocktail consists of various enzymes, including endoglucanase, cellobiohydrolase,

and  $\beta$ -glucosidase. The enzymatic process involves a sequential action of these enzymes on the cellulose structure. Endoglucanase primarily targets the amorphous regions of cellulose chains, leading to the cleavage of the  $\beta$ -1,4-glycosidic bonds and reducing the size of the cellulose chains. Cellobiohydrolase acts on the ends of the cellulose molecules to remove the crystalline regions. Finally,  $\beta$ -glucosidase hydrolyses the cellulose into glucose.<sup>85,86</sup> Hence, the careful selection of enzymes becomes crucial to tailor the properties of the resulting nanocellulose. Fig. 5 illustrates the various methods used for extracting nanocellulose.

The enzymatic treatment offers two distinct approaches for recycling blended textile waste containing cellulose. Firstly, it can be employed to separate the cellulose components, like cellulose, from the blend containing non-cellulosic fibers such as polyesters and other materials. Alternatively, this treatment can be utilized to produce bio-based products by breaking down cellulose into sugars, which can then undergo fermentation or other processes to yield bioethanol or simple glucose. Chen *et al.* isolated nanocellulose from cotton pulp fibers using cellulase hydrolysis. They investigated the effects of cellulase concentration and reaction duration on the properties of the nanocellulose. The study revealed that at low cellulase concentrations (10–100  $\mu\text{mol ml}^{-1}$ ), ribbon-like nanocellulose with lengths of 250–900 nm and diameters of 30–45 nm could be obtained. With higher cellulase concentrations (above 100  $\mu\text{mol ml}^{-1}$ ), granular nanocellulose was observed. In addition, the duration of cellulase hydrolysis affected the length but not the diameter of the nanocellulose.<sup>84</sup> A study conducted by Gholamzad *et al.* (2014) shows the ability to retrieve 98% of the PET and a substantial quantity of ethanol (yielding 70%) from cellulose.<sup>87</sup> This was achieved by utilizing enzymatic hydrolysis after initial chemical treatment using various alkali solutions. In this investigation, two different enzymes, which were glucosidase and cellulase, were used to process the cellulose. Biological methods are more suitable for nanocellulose extraction from textile fibers due to their eco-friendly nature and ability to operate under mild conditions, resulting in high-purity nanocellulose. However, these methods can be costly due to the high price of enzymes and face challenges in scaling up microbial fermentation processes, potentially leading to slower production rates. Table 2 outlines the advantages and disadvantages of different nanocellulose extraction methods.

## 4. Utilizations of nanocellulose in the textile industry

The rapid growth in global population has had a notable impact on resource availability, primarily driven by the increased in textile production, leading to potential issues of excessive use and waste generation. Using textile waste fibers for nanocellulose production has its pros and cons compared with using virgin cotton. Textile waste, particularly cotton with its high cellulose content, provides a sustainable and cost-







**Table 1** Current extraction method for pure cotton and cotton blend textile waste to nanocellulose

Textile source	Isolation method	Parameter conditions	Crystallinity Index/%	Size/nm	Yield/%	Results	Ref.
Waste cotton cloth	Chemical (alkaline pre-treatment, acid hydrolysis), mechanical	10% NaOH for about 2 h hydrolysis: H <sub>2</sub> SO <sub>4</sub> and HCl at 55 °C for 7 h using ultrasonic waves	55.76 ± 7.82	Length: 28–470 Diameter: 3–35	46.7	The crystallinity is significantly high, but the thermal stability is lower in comparison to the original material	38
Cotton-polyester (70 : 30) blend	Chemical (acid hydrolysis), mechanical	H <sub>2</sub> SO <sub>4</sub> solution at 90 °C for 40 min. Polyester fiber was ground by a grinder and passed through an 80-mesh sieve to separate the two compositions	91	Length: 214.6–234.6 Diameter: 23.7	89.5–98.2	PET was gathered in the sieve, while cotton powder was accumulated in the collector. The cotton was then employed to isolate NCC for composite applications	46
Indigo-dyed denim fabric	Chemical (acid hydrolysis, TEMPO oxidation), mechanical	Initial size reduction using a cutting mill, followed by 64% H <sub>2</sub> SO <sub>4</sub> at 45 °C for 1 h, ultra-sonication, and TEMPO/NaBr/NaClO used at pH 10–10.5 for 6.5 hours. Microfluidization was performed with 5 passes at 30 000 psi	66–86.4	Length: 127.7 ± 43.8–175.2 ± 93.0 Diameter: 9.90 ± 3.8–12.5 ± 4.3	37.8–78.9	Greater crystallinity and improved thermal stability compared with the original material. However, fiber discoloration occurred due to inadequate bleaching	50
Cotton waste	Chemical (oxidation bleaching, acid hydrolysis), mechanical	Bleaching involved 4 h at 60C with NaOCl <sub>1</sub> followed by 30–50% H <sub>2</sub> SO <sub>4</sub> and additionally sonication was conducted for 45 min using an ultrasound probe sonicator	81.23	50	—	Higher thermal stability when compared with the original material. However, the process is less cost-effective when measured against the yield	51
Industrial cotton wastes	Chemical (acid hydrolysis)	60% H <sub>2</sub> SO <sub>4</sub> used at 50 °C for 8 h using 60% compositions	—	Length: 180 ± 60 Diameter: 10 ± 1	45	Distinctive fluorescence properties make it suitable for bioimaging. However, high energy and time consumption are needed	54
Viscose fibre textile waste	Chemical (APS oxidation)	APS at 70 °C–100 °C for 2–10 h	51.3–80.4%	34–49	37.89–39.91	NCC can serve as an effective emulsion stabilizer due to its high thermal stability. However, a reaction time exceeding 6 h disrupts the crystalline structure	58
Denim Waste	Chemical (alkaline treatment, APS oxidation)	Alkali pretreatment for 3 h using NaOH. Oxidation using ammonium persulfate (APS) at 60 °C for 5 h	83	Length: 76.14 ± 8.56 Diameter: 18.10 ± 3.54	21.46–27.24	Reduced reaction time but reduced crystallinity due to APS concentration	59
Waste cotton cloth	Chemical (alkali pre-treatment, acid hydrolysis), mechanical	NaOH pre-treatment, H <sub>2</sub> SO <sub>4</sub> /HCl hydrolysis (65 °C, 5 h) and high-intensity ultrasonication	—	Length: 38–424 Diameter: 2–17	49.2 ± 1.6	NCC exhibits uniform fiber diameter, a dense network, and high crystallinity, which prevents the formation of a transparent film on its surface when compared with the precursor material	74
Cotton textile waste	Chemical (alkaline pre-treatment, chlorine-free bleaching, acid hydrolysis)	Concentrated NaOH solution at 70 °C for 1 hour, followed by a bleaching step at 50 °C for 1 hour using a mixture of H <sub>2</sub> O <sub>2</sub> and NaOH. Then pulp fiber to acid solution ratio of 1 to 20 with H <sub>2</sub> SO <sub>4</sub> at 50 °C	75–81	Length: 203.7 ± 68.6–1819.3 ± 328.5 Diameter: 16.5 ± 3.6–248.0 ± 130.1	62.98–83.03	Efficient pretreatment effectively eliminates the amorphous dye colors from textiles, but it decreases the practicality of its application due to the elevated costs stemming from the slower reaction rate	75
Cotton linter	Chemical (alkaline pre-treatment, acid hydrolysis)	NaOH at 50 °C for 24 h, H <sub>2</sub> SO <sub>4</sub> hydrolysis	82	Length: 133 Diameter: 10	59–72%	Reduced water retention capacity when compared with the original material is attributed to the lower crystallinity from fiber degradation that is caused by the acidic concentration	76
Textile cotton gin waste	Chemical (acid hydrolysis)	H <sub>2</sub> SO <sub>4</sub> solution at 55 °C for 60 min	>78%	Length: 100–300 Diameter: <10	50%	Improved thermal stability and increased crystallinity in contrast to the original material. However, the yield is low	77
Cotton-polyester blend	Chemical (alkaline treatment, acid hydrolysis), mechanical	NaOH treatment, 64% H <sub>2</sub> SO <sub>4</sub> and high-pressure homogenization	79.39	Length: 40–400 Diameter: 40–100	—	NCC were obtained and PET was recovered	78
Pure cotton and cotton-polyester (50–:50) blend	Chemical (TEMPO oxidation), mechanical	Microgrinding, TEMPO/NaBr/NaClO oxidation at pH 10–10.5 by using 0.1M NaOH	65–83	Diameter: 10	73 ± 5.2–77 ± 3.4	NCC obtained with high crystallinity index of about 80% and size less than 6 nm	79

Table 1 (Contd.)

Textile source	Isolation method	Parameter conditions	Crystallinity Index/%	Size/nm	Yield/%	Results	Ref.
Cotton textile waste	Chemical (alkaline treatment, ozone bleaching, acid hydrolysis), mechanical	25% NaOH with 0.2% anthraquinone at 160 °C for 4 h and ozone bleached (gas flow rate of 0.5 L min <sup>-1</sup> at 30 °C). Supercritical CO <sub>2</sub> explosion (2 h at 500 bars at 60 °C) & high-pressure homogenization	—	Length: 60–220 Diameter: 10–30	—	NCC obtained with high crystallinity and incorporated with poly(lactic acid), chitin to enhance thermomechanical properties for packaging application. Involves multiple processing and chlorine-free bleaching	80
Viscose-rayon and nylon yarn	Chemical (acid hydrolysis), mechanical	64 wt% H <sub>2</sub> SO <sub>4</sub> at 40 °C for 30 min, ultrasonicated	—	Diameter: 65.03 ± 10.15	—	NCC powder as a green nanofiller was extracted from the viscose-rayon textile yarn waste by acid hydrolysis and later introduced into the nylon matrix obtained from nylon textile yarn waste	81
Cotton-polyester (65 : 35) blend	Chemical (alkaline treatment, acid hydrolysis)	20% NaOH at 85 °C for 2–4 h, then the material was added into 60% H <sub>2</sub> SO <sub>4</sub> at 45 °C for 1.30 h	—	—	56.26	NCC were obtained and blended with PVA and silver nanoparticles to form biodegradable film composites	82
Raw and bleached cotton sliver	Chemical (acid hydrolysis), mechanical	64% H <sub>2</sub> SO <sub>4</sub> at 45 °C for 45 min, ultrasonication	85–89.88	Length: 130–300 Diameter: 8–34	78.1 ± 0.05–88.4 ± 0.12	NCC were obtained and used in nanocomposite films with sodium alginate.	83
Cotton pulp fiber	Biological (enzymolysis)	Swelling with glycerine, cellulase hydrolysis	—	Length: 250–900 Diameter: 30–45	—	Ribbon-like CNC produced	84

effective raw material for efficient nanocellulose production, aligning with waste management and circular economy principles. However, the diverse nature of textile waste necessitates thorough pre-treatment processes due to various fiber types and contaminants, presenting environmental and economic challenges. Additionally, cotton from secondary waste may have reduced mechanical properties, underlining the need to optimize nanocellulose properties by combining it with other fibers for diverse applications. Studies focusing on nanocellulose from textile waste have conducted technical assessments to evaluate the chemomechanical properties. Despite differences in functionality between virgin and recycled nanocellulose, utilizing recycled nanocellulose in the textile industry can reduce the demand for virgin fiber production, thus mitigating environmental impacts.

#### 4.1. Filtration

Conventional processes involved in textile manufacturing often result in some environmental concerns, particularly in the areas of dyeing and heavy metal pollution.<sup>90–92</sup> To address these issues, researchers have turned their attention to the potential application of nanocellulose in the textile industry, exploring its application in the filtration processes for the removal of dyes and heavy metals from textile wastewater.

In today's context, the removal of dyes from textile wastewater is a pressing concern, as the textile industry is one of the major contributors to water pollution due to the discharge of dye-containing effluents.<sup>93,94</sup> Traditional methods for dye removal, such as chemical precipitation, chemical oxidation, adsorption and coagulation, are often inefficient and costly, and generate significant amounts of sludge.<sup>95,96</sup> Nanocellulose-based filtration systems provide a promising alternative by effectively adsorbing and removing dyes through physical and chemical interactions,<sup>97</sup> offering the potential for efficient and sustainable dye removal processes.

In a recent work by Tavakolian *et al.*, hairy nanocellulose, a biorenewable and easily functionalized form of cellulose nanoparticles, was investigated due to its potential as an effective, low-cost adsorbent.<sup>98</sup> Electrosterically stabilized nanocrystalline cellulose (ENCC), a variant of hairy nanocellulose with a notably high negative charge density, holds significant promise for dye adsorption. The group focuses on ENCC's efficacy in removing cationic dye methylene blue from wastewater, revealing its remarkable removal capacity of up to 1400 mg g<sup>-1</sup>. This work highlights ENCC's aptitude for dye removal under varying conditions, investigating the impacts of factors like ionic strength and pH. The study also reported an innovative approach involving the integration of ENCC into sodium alginate hydrogel beads (ALG-ENCC beads), enabling easier application on a larger scale without the need for separate filtration steps. ENCC's versatility extends beyond dye removal, suggesting potential for addressing various forms of contaminated wastewater, including positively charged contaminants such as heavy metals. The composite ALG-ENCC beads exhibit a superior maximum adsorption capacity compared with ALG-only beads, attributed to their composition of 50%



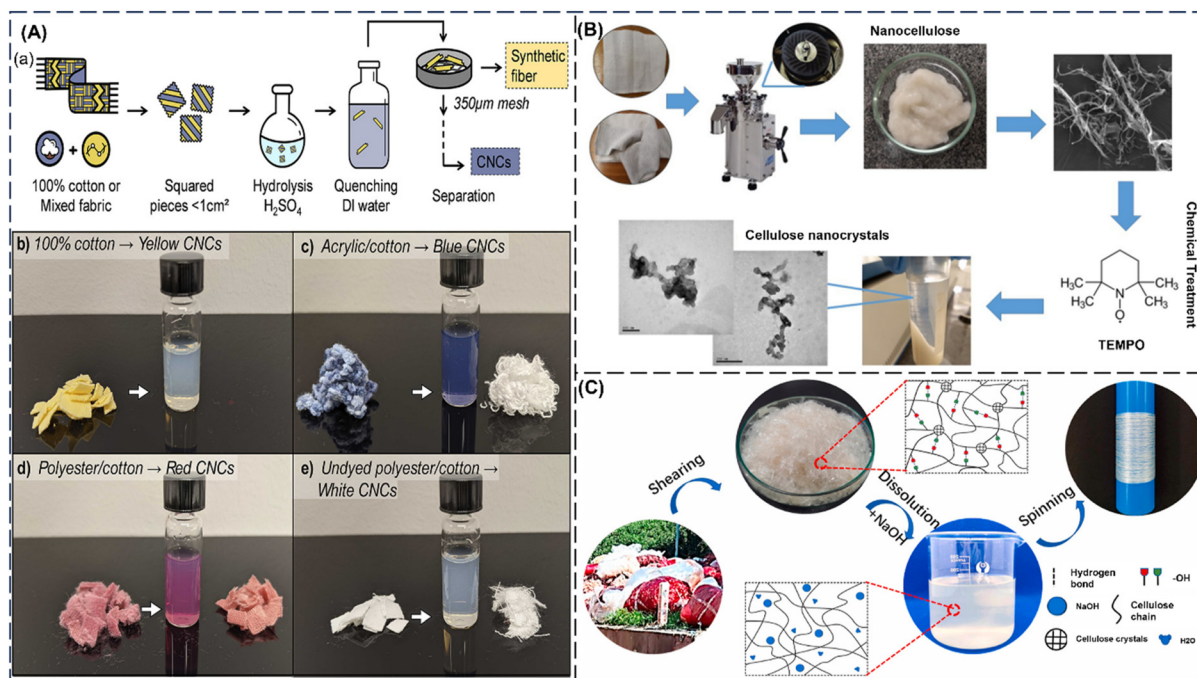


**Fig. 5** Extraction methods of nanocellulose. (A) Flow chart of nanocellulose from 100% cotton or blends by (a) acid hydrolysis. (b–e) left of arrows, images of postconsumer fabrics used in this work; right side of arrows, the resulting products after hydrolysis, which include nanocellulose extracted in suspension form and recovered synthetic fibers (adapted with permission from ref. 88). Copyright 2022 ACS Publications. (B) Process flow chart of nanocellulose from 100% cotton and polyester-cotton blends by wet milling and TEMPO oxidation. Adapted with permission from ref. 79. Copyright 2021 Springer. (C) A schematic diagram of cellulose dissolution from viscose films in NaOH aqueous solution to generate RCF. Adapted with permission from ref. 89. Copyright 2021 Elsevier.

**Table 2** Advantages and disadvantages of extraction methods used for nanocellulose

Physical and mechanical method	Chemical method	Biological methods
<b>Advantages</b> <ul style="list-style-type: none"> <li>Relatively simple and cost-effective method for producing nanocellulose.</li> <li>Can yield nanocellulose with high aspect ratios and specific surface areas.</li> <li>Does not involve the use of chemicals, making it environmentally friendly.</li> </ul> <b>Disadvantages</b> <ul style="list-style-type: none"> <li>Limited in its ability to modify the chemical properties or functional groups of nanocellulose.</li> <li>Requires high energy input, which can lead to increased production costs.</li> <li>May result in mechanical damage or reduction in crystallinity, affecting the properties of nanocellulose.</li> <li>Limited control over surface chemistry or functionalization compared with chemical treatments.</li> </ul>	<ul style="list-style-type: none"> <li>Can efficiently remove impurities and modify the properties of nanocellulose.</li> <li>Allows for precise control over surface chemistry and functionalization.</li> <li>Enables the production of various types of nanocellulose with tailored properties.</li> <li>Energy intensive.</li> <li>Requires careful handling and disposal of chemicals to minimize environmental impact.</li> <li>Requires toxic chemicals and generates hazardous waste as reaction by-product.</li> <li>Not eco-friendly.</li> </ul>	<ul style="list-style-type: none"> <li>Utilizes enzymes or microorganisms to break down cellulose into nanocellulose, which can be more environmentally sustainable.</li> <li>Offers potential for mild and specific modifications of nanocellulose properties.</li> <li>Can be integrated into bio-refinery processes for efficient resource utilization.</li> <li>Requires optimization of enzyme or microbial activity for efficient nanocellulose production.</li> <li>Process may be slower compared with chemical or mechanical methods.</li> <li>May have limitations in terms of scalability and industrial application.</li> </ul>

alginate and 50% ENCC, presenting a handling advantage over ENCC alone due to ease of separation by gravity, thus offering a promising solution for scalable applications (Fig. 6A).

In another work, Amiralian *et al.* presented a compelling avenue in the realm of dye removal from wastewater.<sup>101</sup> The

investigation focuses on synthesizing magnetic nanoparticles through the utilization of cellulose nanofibers as templates, resulting in nanoparticles with diameters less than 20 nm and a uniform size distribution. These magnetic nanoparticles are then affixed onto the nanofiber surfaces *via in situ* hydrolysis





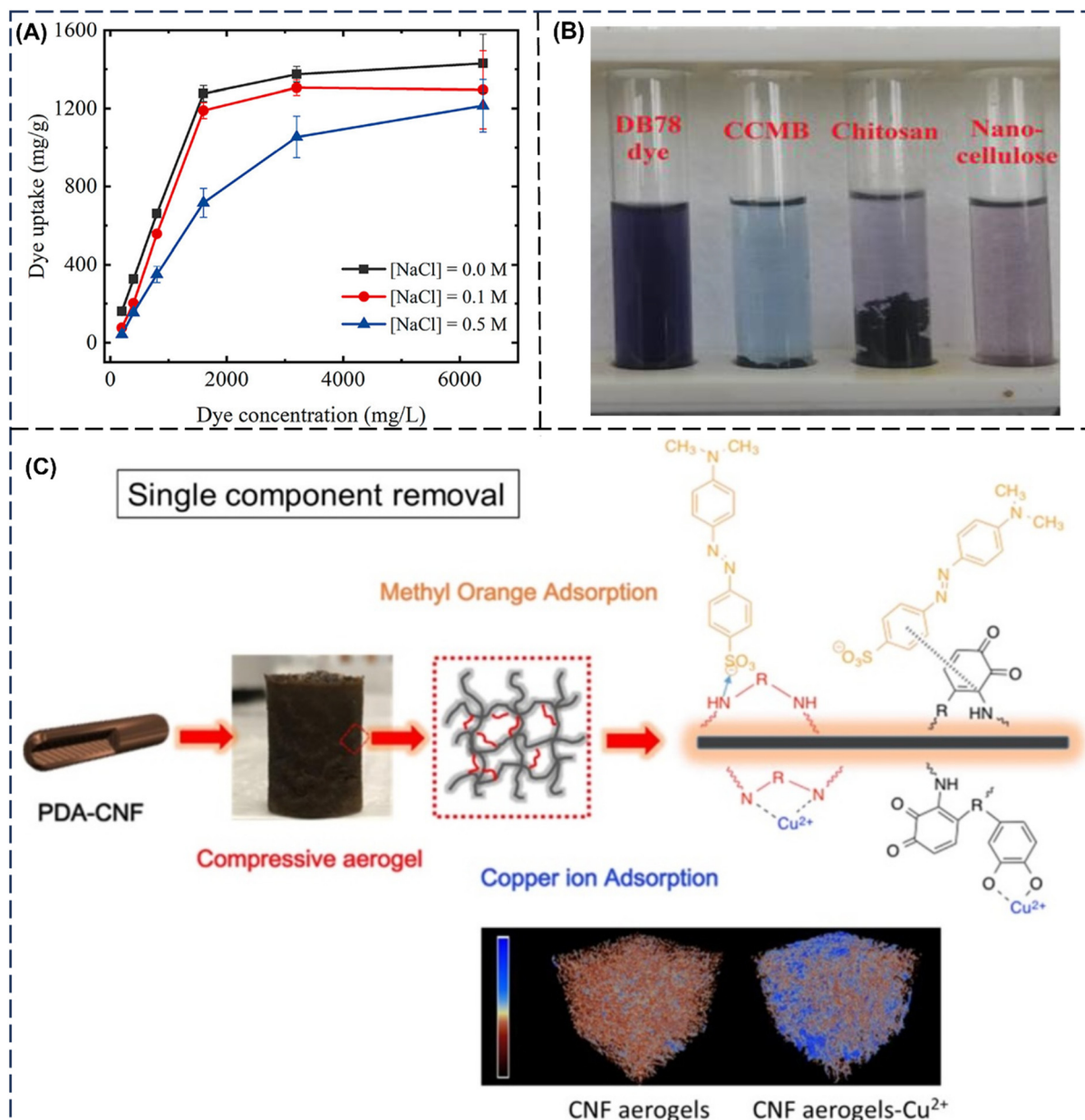


**Fig. 6** (A) Comparison of dye uptake among ENCC alone, 1:1 ALG:ENCC beads, and ALG-only beads at different dye concentrations. Adapted with permission from ref. 98. Copyright 2020 ACS. (B) Adsorption of DB78 dye using chitosan, nanocellulose, and CCMB-0.25:1 adsorbents. Adapted with permission from ref. 99. Copyright 2022 MDPI. (C) Interactions of aerogels with methyl orange (MO) and copper ions (Cu<sup>2+</sup>) for heavy metal and dye removal, including X-ray microtomography images of CNF-based aerogels after Cu(II) adsorption (scale bar: 250  $\mu$ m) and kinetic curve for Cu(II) adsorption by PDA-CNF aerogel adsorbent. Adapted with permission from ref. 100. Copyright 2019 Elsevier.

of metal precursors at room temperature. The research delves into the impact of varying nanofiber concentrations on the resultant magnetic nanoparticle morphology, crystallite size, as well as thermal and magnetic attributes of the produced membranes. These magnetic membranes, boasting a high concentration of magnetic nanoparticles, exhibit superparamagnetic behavior and impressive magnetic properties, establishing their efficacy. Remarkably, these magnetic membranes showcased a remarkable 94.9% degradation of rhodamine B, a prevalent hydrophilic organic dye utilized in industry, within

just 300 minutes at room temperature. This work underscores the successful synthesis of magnetic nanoparticles *via* cellulose nanofibers, offering valuable insights into nanoparticle formation and growth mechanisms.

In the context of wastewater treatment, the efficient removal of anionic dyes from industrial effluents remains a pressing concern due to their adverse environmental impacts and potential health hazards. More recently, Bassyouni and team utilised nanocellulose for anionic dye removal from textile industrial wastewater.<sup>99</sup> Nanocellulose was extracted from





palm leaves, and was subsequently employed to form nanocellulose/chitosan nanocomposites. The potential of chitosan, nanocellulose, and the novel synthetic nanocellulose/chitosan microbeads (CCMB) for the removal of direct anionic blue 78 dye was evaluated through batch experiments, encompassing various parameters such as adsorbent concentration, mixing time, pH, and dye initial concentration. Remarkably, the synthesized CCMB demonstrated a surface area of  $10.4 \text{ m}^2 \text{ g}^{-1}$  and a positive net surface charge. The adsorption tests exhibited a direct relationship between adsorbent concentration and dye removal efficiency, with maximum removal efficiencies of 91.5% and 88.4% achieved using CCMB-0.25 : 1 (Fig. 6B). The team concluded that the nanocellulose/chitosan ratio 0.5 : 1 was optimal in removal efficiency. Collectively, chitosan, nanocellulose, and CCMB prove to be promising and efficient adsorbents for wastewater treatment, particularly in dye removal applications.

On the other hand, the presence of heavy metals in textile wastewater poses a serious environmental threat. Heavy metals, often used in dyes and textile finishes, can have adverse effects on ecosystems and human health.<sup>102</sup> Conventional treatment methods for heavy metal removal, such as precipitation, membrane filtration, or electrochemical treatment, have limitations in terms of selectivity and reusability.<sup>103,104</sup> Nanocellulose-based filtration systems show promise in addressing these limitations by leveraging the high surface area and adsorption capacity of nanocellulose to selectively capture and remove heavy metal ions from textile wastewater.

Recent advances in nanocellulose research have showcased its potential to serve as an innovative adsorbent in the realm of water treatment. Notably, Li *et al.* reported work which utilised TEMPO-oxidized cellulose nanofiber (TOCNF) heavy metal removal.<sup>105</sup> With rapid adsorption kinetics and remarkable capacities, TOCNFs have proved their efficiency in the removal of Cu(II) and Zn(II) from water sources. The selectivity of TOCNFs, particularly in copper adsorption, underscores their specificity and effectiveness. The elucidation of complex adsorption mechanisms involving ion exchange, coordination, and accumulation further establishes their potential for sustainable water reclamation.

Parallel to these developments, cellulose nanofibril (CNF) based aerogels have gained prominence as a sustainable and efficient approach to heavy metal removal from wastewater. Tang *et al.* developed CNF-based aerogels through innovative mussel-inspired coating strategies,<sup>100</sup> exhibiting outstanding adsorption capabilities, especially in the context of Cu(II) and methyl orange (MO) contaminants (Fig. 6C). The controlled synthesis process results in aerogels with low density, high porosity, and robust 3D networks, setting the stage for effective heavy metal adsorption. The high adsorption capacities revealed by these aerogels underpin their potential as practical solutions for sustainable wastewater treatment. These works emphasize nanocellulose's versatile role in addressing multifaceted challenges within the textile industry, ranging from heavy metal ion to dye removal.

## 4.2. Dye technology

Nanocellulose offers a potential solution for enhancing the fixation of reactive dyes and reducing dye discharge in textile dyeing processes.<sup>106,107</sup> Nanocellulose's large surface area and the ability to form stable suspensions make it an ideal candidate for efficient dye adsorption and retention.<sup>107,108</sup> By integrating nanocellulose into the dyeing process, it has the potential to improve dye fixation by promoting stronger interactions between the reactive dyes and the fabric. Additionally, nanocellulose also acts as a binder which helps to anchor the reactive dyes onto the fabric and prevents their leaching during subsequent washing or sweating.<sup>106</sup> This in turn reduces the risk of colour fading and bleeding, ensuring that the fabric retains its vibrant appearance for an extended period, and reduces dye discharge into wastewater, thus minimizing environmental pollution.

A polyester substrate, composed entirely of 100% polyester, was subjected to treatment using a CNC suspension derived from remnants of viscose rayon fibers. These suspensions were dyed using a direct dye such as Congo red BDC.<sup>109</sup> The application of CNCs boosted the color intensity of the polyester fabric and enhanced its resistance to soaping. The research illustrated that the application of CNCs on polyester fibers resulted in an improvement in their resistance to mechanical loading. The enhancement in physical and mechanical characteristics was credited to the mechanical interlocking generated by the presence of CNCs within the intermolecular pores of the polyester.

Conventional dyeing processes, such as indigo dyeing for denim fabrics, have been associated with significant water consumption, utilization of toxic reducing agents, and the release of alkali-laden effluents into wastewater. However, a novel indigo-dyeing technology has been recently developed by Rai and team, leveraging the high surface-to-volume ratio of nanocellulose.<sup>110</sup> This innovative approach drastically reduces water consumption by up to 25 times, eliminating the need for harmful reducing agents and alkali, while enhancing dye fixation to over 90%, surpassing the conventional dyeing efficiency. This simplified process involves depositing a nanocellulose hydrogel loaded with natural indigo particles and chitosan onto cotton denim fabric or yarn (Fig. 7A). The resulting nanofibrillated cellulose mesh-like coating encapsulates the indigo particles, and chitosan acts as a cross-linker, improving fixation and adhesion. Post-treatment with chitosan further enhances the dyeing performance, offering superior color strength, and maintaining fabric comfort properties. This technology not only demonstrates the potential to revolutionize denim dyeing but also presents a scalable and adaptable solution for various textile dyeing applications, contributing to reduced chemical usage, energy conservation, and efficient water management in the textile industry.

By utilizing NFC hydrogels infused with reactive dyes, Liyanapathirana *et al.* presented a revolutionary dye carrier that significantly curtails water consumption and auxiliaries, contributing to a 6-fold reduction.<sup>107</sup> Cotton fabrics and NFC hydrogels inherently contain soluble polysugars that bind with



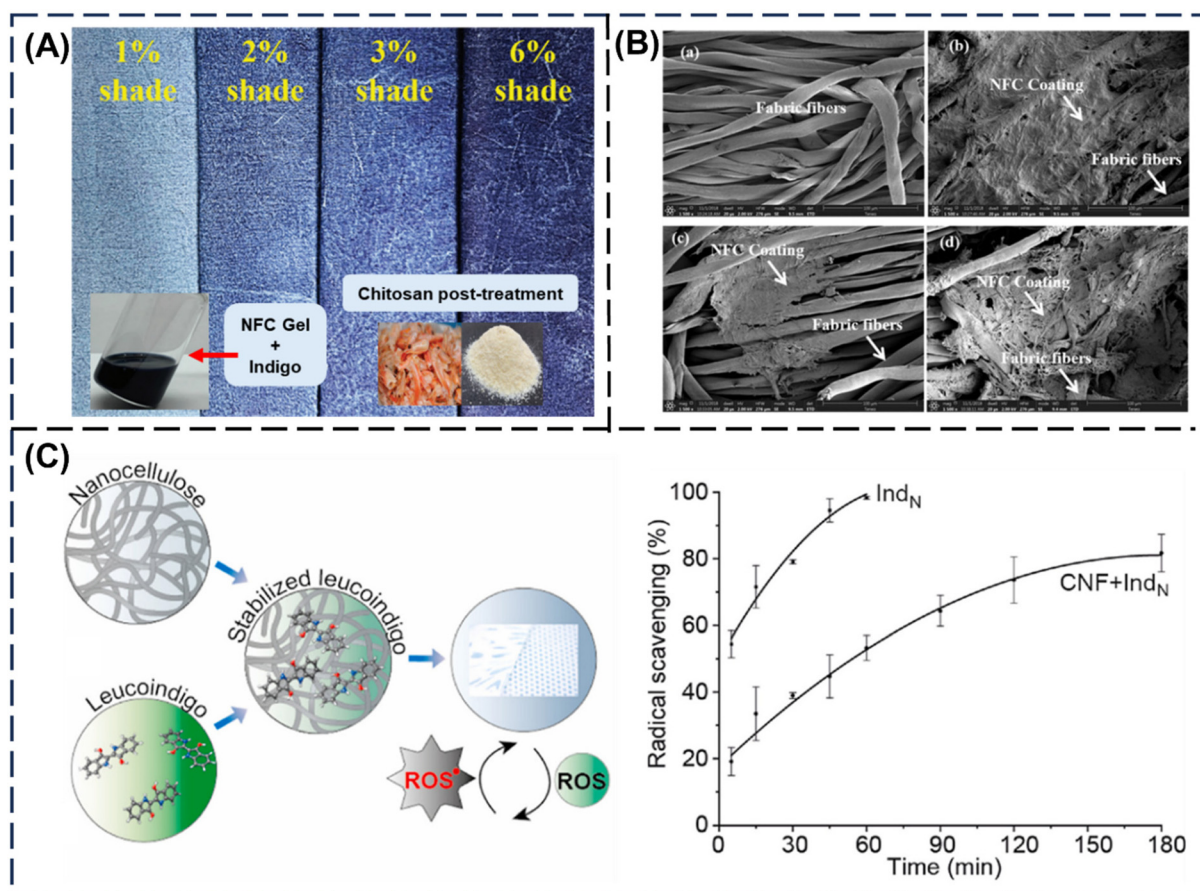


**Fig. 7** (A) Cotton fabric dyed with NFC-indigo and chitosan post-treatment. The percentage shade indicates the indigo pigment weight relative to undyed cotton textile. Adapted from ref. 110. Copyright 2021 Royal Society of Chemistry. (B) SEM images at 1500 $\times$  magnification: (a) untreated cotton fabric, (b) NFC-dye coating before washing, (c) NFC-blue dye-coated fabric after 5 wash cycles, and (d) NFC-blue dye-coated fabric with PCA post-treatment, demonstrating coating retention after 5 wash cycles. Adapted from ref. 107. Copyright 2020 ACS Publishing. (C) Schematics on the stabilisation of leucoindigo on nanocellulose for simplified processing and cotton printability, with radical scavenging activity compared between natural indigo and indigo nanocellulose film. Adapted with permission from ref. 111. Copyright 2021 Elsevier.

reactive dyes, leading to water pollution and reduced dyeing efficiency. The study unveils a post-treatment strategy involving polycarboxylic acid (PCA) that facilitates the permanent grafting of dye-labeled polysugars, forming chemical cross-links with NFC fibers on cotton fabric (Fig. 7B). This breakthrough enhances dye fixation by 30% and diminishes dye discharge by 60%, all while preserving fabric attributes like stiffness and breathability. The approach was found to be versatile, tested across an array of reactive dyes, and governed by factors such as temperature, NFC concentration, and the type of PCA employed. This research highlights the potential of nanocellulose-driven innovations in revolutionizing textile dyeing processes, ushering in a more sustainable era for industry.

In a related work, Lohtander *et al.* focuses on the stabilization of leucoindigo, the soluble form of natural indigo derived from *Isatis tinctoria*, on a nanocellulose carrier.<sup>111</sup> Typically, indigo dyeing necessitates complex conversion processes between its soluble and insoluble forms, often involving harsh chemicals. This work introduces an innovative approach where the leucoindigo form is stabilized on a nanocellulose

matrix, avoiding the need for repeated re-reduction steps and harmful chemicals (Fig. 7C). Spectroscopic and photophysical analyses confirmed the successful stabilization, attributing it to the restricted oxygen diffusion within the nanocellulose medium. Particularly noteworthy is the extended stability achieved when using natural indigo, which is attributed to the antioxidant properties of this natural dye. This stability-enhancing nanocellulose carrier not only streamlines the dyeing process but also amplifies the value of natural dyes through novel functionalities. The findings offer an environmentally friendly solution to traditional dyeing challenges, shedding light on the promising role of nanocellulose in sustainable textile practices.

In conclusion, nanocellulose stands as a transformative agent in the drive for sustainable textile practices, particularly in dye fixation and leaching prevention. As presented by recent research work, its exceptional surface area and stabilizing properties offer a dual advantage of enhancing dye adhesion while preventing environmental leaching. These attributes hold the promise of revolutionizing traditional dyeing



methods, minimizing water consumption, reducing chemical usage, and contributing to the broader goals of eco-friendly textile production. Despite its potential, the integration of nanocellulose into the textile industry for enhanced dye fixation and leaching prevention warrants continued exploration, considering scalability, cost-effectiveness, and broader industrial implications.

### 4.3 Textile coating and reinforcement of nanocellulose in textile fibers

By exploiting its surface chemistry and nanoscale, nanocellulose can contribute to a range of benefits such as reinforcement onto fabrics or fibres, development of barrier coating for protection and functionalization of textiles. nanocellulose can enhance these materials in terms of their mechanical properties, resistance, wettability, and thermal stability. This can be valuable for the restoration and protection of textile pieces such as painted canvases and tapestry. Precious artworks will degrade over time due to continuous exposure to humidity and temperature.<sup>112</sup> The degradation results in permanent damage to the artworks and can be identified by cracks in the fibres and depolymerisation of cellulose at the nanoscale.<sup>113</sup> Restoration works can be challenging as choice of treatment and chemical exposure can be complex and detrimental to the artwork.

Current conservation efforts are largely on reinforcement of the microenvironment in the canvas rather than repair. Briefly,

the traditional restoration method involves an adhesive layer followed by a new canvas layer lined at the back.<sup>114</sup> However, as most canvases are cellulose-based, the use of water-based adhesives can be a concern due to its moisture sensitivity and synthetic-based films can be toxic in the long run. Structural reinforcements are necessary to maintain and prevent further degradation of the canvas. This can be made with the different nanoscale cellulose, such as nanofibrils (CNF), cellulose nanocrystals (CNC), and carboxymethylated cellulose nanofibrils (CCNF), in the degraded canvas. Diluted suspensions of CNF, CNC and CCNF were deposited onto the degraded canvas, which results in a film formation, like the current conservation methods. Amongst the three different types, CNF holds better potential in long-term stability due to the absence of acid groups.<sup>115</sup> The group had also explored multi-layer treatment with CNF and polyamidoamine-epichlorohydrin (PAAE) as a film restoration coating.<sup>116</sup> The PAAE plays an important role in coupling the canvas fibres and improving the reinforcement of CNF. The PAAE polymer is commonly used to improve the mechanical properties of paper in wet conditions through the increase in crosslinking and inter-fibre adhesion of cellulose.<sup>117</sup> Fig. 8A and B demonstrates the different morphology of the canvas fibres and their corresponding mechanical properties when treated with CNF, PAAE and PAAE/CNF. The addition of PAAE can facilitate the anchoring of CN on the canvas but would still need further optimization due to its

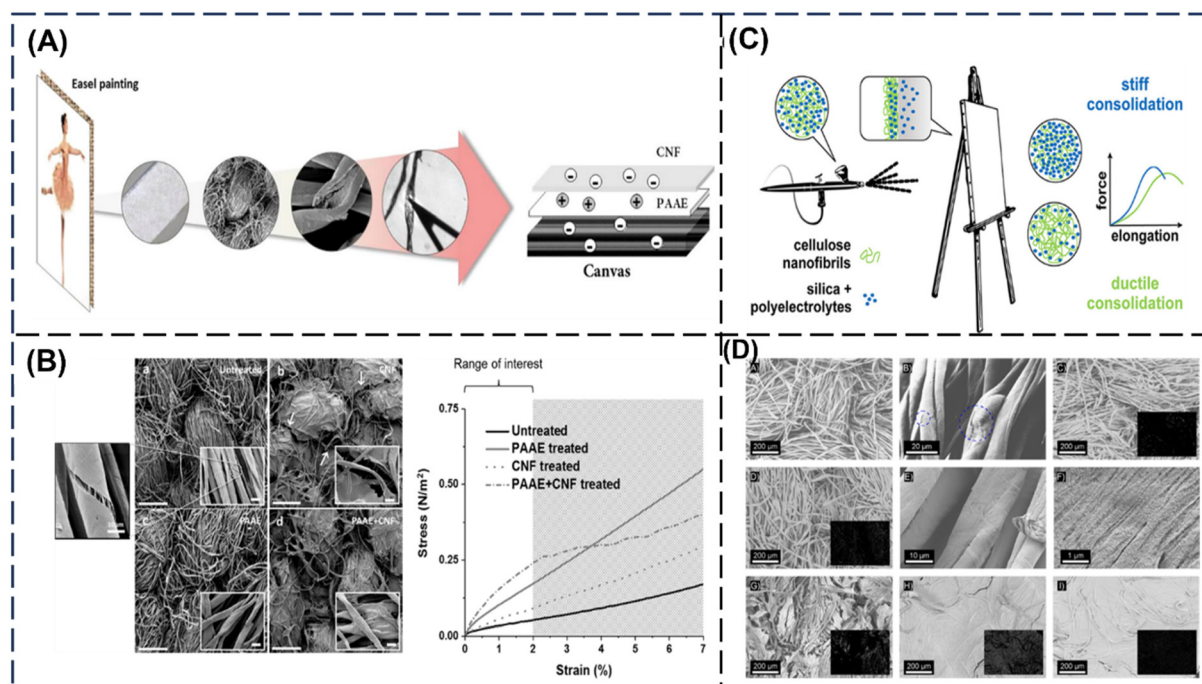


**Fig. 8** (A) The schematic of canvas restoration with CNF and PAAE as an intermediary layer. (B) SEM images showing the deposition of the treatment onto the surface of (a) untreated canvas, (b) CNF-treated canvas, (c) PAAE-treated canvas, and (d) PAAE/CNF-treated canvas, and the increase in mechanical properties after treatment. This is reprinted from © 2022 American Chemical Society.<sup>116</sup> (C) The integration of SNP and CNF results in a tuneable stiffness and ductility in the canvas. (D) The corresponding SEM pictures of degraded cotton canvas (A and B) before and after treatment with (C) silica, (D–F) CMC@SNP, and different CMC@SNP : CNF with mixtures of (G) 9 : 1, (H) 1 : 1, and (I) 1 : 9 after application of two layers of each formulation. The insets show the results of EDX analysis of silica abundance on the surface of the investigated samples. The dashed circles indicate cracks on the surface of the fibers. These are adapted from © 2022 American Chemical Society.<sup>118</sup>





responsiveness to moisture. In a similar approach, polyelectrolyte-treated silica nanoparticles (SNP) were combined with CNF as a deposition onto the canvas (Fig. 8C). As CNF and the canvas have a similar chemical nature but not with SNP, polyelectrolyte multilayers were prepared using poly(ethylenimine) (PEI) and carboxymethyl cellulose (CMC) to better the interactions. The alterations between the CNF and SNP content varied the effects on the canvas whereby the increase in CNF resulted in a ductile behaviour and the addition of SNP a stiffer behaviour. However, both approaches can tackle the loss of structural integrity in the canvas.<sup>118</sup>

In recent years, hybrid efforts with CNC had also been explored not only with cellulose canvas but also silk artifacts. Historical silk textiles such as tapestry, clothing and décor can degrade by hydrolysis and oxidation with exposure to the environment or even be chemically altered from microorganisms. The conservation efforts of these have been reparation with synthetic adhesives which can be more damaging in the long run.<sup>119,120</sup> Ciani *et al.* fabricated a composite of CNC and self-regenerated silk fibroin (SRSF) colloidal dispersion to increase the structural stability of aged silk fibres.<sup>121</sup> The addition of SRSF/CNC increases the axial force at break and maintains the original elongation of the degraded fibres. The exposure of UV onto the silk fibres exposed it to oxidation and chemical modifications that resulted in disordered domains. The composite was able to shield this better than its individual components and has proved to be crucial to the aging of silk textiles against sunlight exposure.

The addition of nanocellulose to textiles can further enhance textile properties in terms of thermal resistance and mechanical strength. This is useful not only to canvas restoration and repair but also to develop functional and enhanced textiles for use in different industries. Cellulose nanowhiskers (CNW) were developed and applied to polyester textiles to evaluate their contribution to the behaviour of the material.<sup>122</sup> While the increase in thermal resistance is minimal, CNW was able to enhance the colour absorbency and retainment of the dye on polyester fabric after washing. The addition of CNW did not alter the feel and stiffness of the fabric. The nanoscale cellulose can also facilitate the change in surface properties of the fabric, altering its wettability. Cheng *et al.* developed an integration of an adhesive, epoxidized soybean oil (CESO), a structure contributor, CNC and a modifier for lowering surface energy, hexadecyltrimethoxysilane (HDTs), on to a cotton fabric for oil/water separation.<sup>123</sup> The superhydrophobic and degradable fabric can separate oil and water with 98% efficiency, comparable to other oil/separation systems. The fabric also demonstrates excellent resistance to alkali and acid exposure. The superhydrophobic cotton cloth can potentially address the need for greener alternatives in oil/water separation systems. In addition, functionalized nanocrystalline cellulose (NCC) with cations can modify the surface of polyethylene terephthalate based fabric and increase its hydrophilicity.<sup>124</sup> The surface of the NCC was quaternized by grafting glycidyl tri-methyl ammonium chloride (GTMAC) and subsequently applied onto the fabric using a commercial binder.

The resulting fabric had a significant improvement in its hydrophilicity and durability due to the unique qualities of NCC that consists of dense polar groups and the quaternization that further enhances both qualities.

The NCC coating naturally improves the mechanical attributes of the textile it covers by leveraging its biocompatibility and non-toxic characteristics. This makes CNF coating a feasible choice for smart textiles employed in medical devices such as lumbar belts.<sup>125</sup> These protective devices are crucial for preventing and mitigating the risk of spine injuries during intense workloads or when workers fail to take adequate care while executing their duties. An ideal fabric should adapt to varying conditions such as pressure, load, humidity, and temperature. Samples of poly(ethylene terephthalate) were coated with CNFs and potato starch gel. Starch was used to enhance the adhesion of the CNF coating to the polyester substrate. While the water-soluble property of the coating makes it inappropriate for protective garments because of starch solubility, traction tests showed a notable rise in elasticity when the textile was infused with nanocellulose and starch. Therefore, the CNF coating offers an attractive approach to improving the mechanical characteristics of smart fabrics, given that a suitable anchoring method on synthetic fibers such as PET is established.

Zhang *et al.* prepared a superhydrophobic spray and sprayed it onto different substrates to form superhydrophobic coatings, such as paper, cotton, and polyurethane, to make them waterproof.<sup>126</sup> They anchored octadecyl chains on the surface of cellulose nanocrystals (CNCs) *via* the oxidation self-polymerization of tannic acid (TA) and the Michael addition/Schiff base reaction between polytannic acid (PTA) and octadecylamine (ODA) (Fig. 9A). Then the ODA-PTA@CNCs could be well dispersed in ethanol, forming a sustainable, versatile, convenient, rapid dry, and superhydrophobic CNC ethanol spray. As shown in Fig. 9A, the ODA-PTA@CNC could be sprayed on a variety of hydrophilic substrates to form superhydrophobic coatings, such as printing papers, airlaid papers, polyurethane (PU) sponges, filter papers, and cotton textiles. Moreover, as ethanol was employed as the dispersion solvent, the superhydrophobic ODA-PTA@CNC coating could be formed in less than 30 s after spraying, making it a facile and promising approach for many applications. As shown in Fig. 9A, pristine cardboard is easily wetted by water, while ODA-PTA@CNC-coated cardboard is water-repellent. The tensile strength of filter paper was about 22.7 MPa in the dry state and dramatically reduced to less than 2.5 MPa after being wetted by a drop of water. Due to water repellency, the ODA-PTA@CNC-coated filter paper could not be wetted even after being immersed in water for half an hour and still possessed a similar tensile strength as the pristine filter paper in the dry state (Fig. 9A).

To conquer the fragility of silk, Zhang *et al.* prepared a new regenerated silk fibroin/carbon nanofibers (RSF)/CNF hybrid using the dry-spinning approach through a bioinspired microfluidic chip, which mimicked the shape of spider's major ampullate gland (Fig. 9B).<sup>127</sup> The resulting RSF/CNF fibers





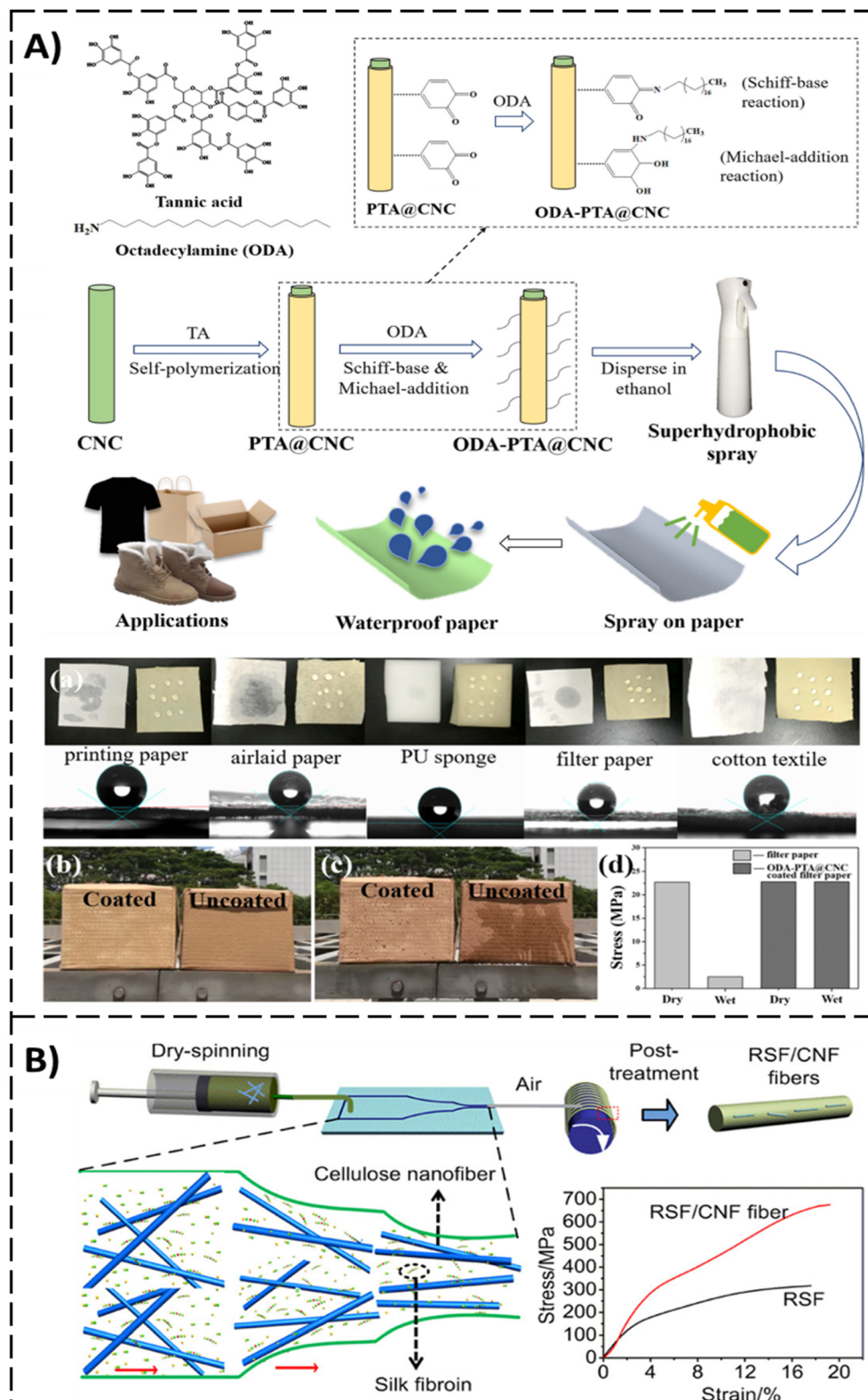


**Fig. 9** (A) Schematic of the facile preparation of sustainable superhydrophobic ODA-PTA@CNCs and their versatile applications. (a) Hydrophilic printing papers, airlaid papers, PU sponge, filter papers, and cotton textile became hydrophobic after being coated with ODA-PTA@CNCs. (b and c) Comparison of pristine and ODA-PTA@CNC-coated cardboards after being splashed with water. (d) Tensile strength of pristine and ODA-PTA@CNC-coated filter papers in the dry and wet state, respectively. Adapted with permission from ref. 126. Copyright 2021 American Chemical Society. (B) Preparation of regenerated silk fibroin (RSF)/CNF hybrid fibers. Adapted with permission from ref. 127. Copyright 2019 American Chemical Society.



exhibited outstanding mechanical strength (mean value: 486 MPa), exceeding that of typical natural silkworm *B. mori* silk (mean value: 360 MPa).<sup>128</sup> Polylactic acid (PLA) and polyhydroxybutyrate (PHB) are biodegradable aliphatic polyesters that are useful for various applications. However, these biopolymers have some limitations related to poor mechanical, low thermal and barrier properties. Chattopadhyay *et al.* applied nanocellulose to polyester textiles by a padding technique to study their physical and thermal properties.<sup>109</sup> Incorporation of nanocellulose (treatment with 10 g L<sup>-1</sup>) increased the breaking load (from 105.6 kgf to 110.5 kgf) and crease recovery angle (148° to 162°) with almost no effect on the rigidity of the material.

Coating textiles with UV-protection properties serves as a vital measure in protecting individuals from the harmful effects of sun exposure, thereby reducing the risk of skin cancer. Such coatings typically incorporate a transparent layer of materials that absorb UV light, which can be either organic or inorganic. Effective UV protection requires strong absorption in the UV range from 290 to 360 nm, with parameters such as the UV protection factor (UPF) and sun protection factor (SPF) used to evaluate the efficacy of protective garments. Nanostructures and natural materials are recognized as effective options for UV protection, with nanomaterials exhibiting high activity and natural materials being safer for human health and the environment. Combining cellulose nanocrystals with UV-blocking additives can create an anti-UV layer, with three types of CNC applied as a potential UV-blocking layer to cotton fabric.<sup>129</sup> In this procedure, chitosan (CS) acts as both a dispersing agent and binder for the CNCs, resulting in the formation of a biodegradable and biocompatible nanocomposite system. Cotton fabrics are submerged in solutions containing CS/CNCs and then treated by padding, with this procedure repeated multiple times to improve the coating effectiveness. The treated fabrics are then dried and cured at 90 °C for 10 minutes to secure the CS/CNCs nanocomposite onto the fabric's surface. Tannic acid is employed as a plasticizer and cross-linker, owing to its polyphenolic structure, which enhances the UV protection capabilities of the coating. All additives used in the process, including chitosan and tannic acid, contribute to enhancing the UV protection provided by the coating. CNFs can also serve as a stabilizing agent for ZnONPs, commonly utilized in UV-protective clothing finishes. Despite their effective shielding properties, ZnONPs tend to aggregate when applied to modified cotton fabrics due to their large surface area. However, the negative charges of hydroxyl and carbonyl groups on the CNFs interact with the Zn through electrostatic forces, mitigating NP aggregation.

Moreover, the structural similarity between CNFs and cotton fabric facilitates intermolecular hydrogen interactions, enhancing the adhesion of ZnONPs to cotton fabrics and potentially preventing NP leaching during laundering.<sup>130</sup> The evolution of self-cleaning textiles, from earlier superhydrophobic materials to more recent photocatalytic ones, has garnered increasing interest. Photocatalytic activity relies on light-induced reactions of oxidation and reduction, leading to the

breakdown of dirt.<sup>131</sup> TiO<sub>2</sub> is a widely used NP due to its excellent photocatalytic properties, and is capable of decomposing dye pollutants. However, NPs applied in textile finishing have shown poor washing fastness due to the polymer coatings used.<sup>132,133</sup> To address this challenge, Kale *et al.* demonstrated that cellulose derived from viscose could coat cotton fabric with TiO<sub>2</sub>NPs, resulting in permanent stiffness, hydrophobicity, and self-cleaning properties.<sup>134</sup>

The growing preference for medical textiles as part of a healthy lifestyle has spurred a rapid expansion in the antimicrobial textiles market, driving extensive research and development efforts. Antimicrobial properties are highly sought after, especially in times of a pandemic, to minimize widespread infections. Nanocellulose have been explored for its value-added properties in polyester fabric for sportswear. The addition of nanocellulose provides excellent antimicrobial properties against *E. coli*, *S. aureus*, *P. aeruginosa*, and *B. cereus*, good UV protection, and tear resistance.<sup>135,136</sup> In addition, Jebali *et al.* developed allicin- and lysozyme-conjugated nanocellulose, ACNC and LCNC, respectively, for textile applications.<sup>137</sup> The ACNC exhibited excellent antibacterial and antifungal properties through damaging the surface enzymes and proteins. Alvarado *et al.* conjugated porphyrin photosensitizers to nanofibrillated cellulose (NFC) and cellulose sheets, covalently, for self-disinfecting activities *via* photoactivation.<sup>138</sup> The work demonstrated the potential photoactivation of NFC to be woven into textiles for an array of applications such as healthcare protective equipment.

Moving forward from canvas restoration, the Bordes research group had also explored the use of CNF coatings to facilitate inkjet printing for E-textiles (Fig. 10A).<sup>139</sup> The plasticized and conductive silver nanoparticle CNF coatings provide flexibility and customized elements but are limited by washing cycles. However, this shows a promising direction for sustainable electronic materials. In addition, nanocellulose was also applied to jute fabrics as the material easily develops bacterial growth and catches fire. To improve the properties of jute fabrics for the textile industry, various jute-based composites were developed. Phosphorylated nanocellulose (P-NC) and chitosan (CS) were developed as a jute biocomposite for antimicrobial and thermal stability.<sup>140</sup> The combination of CS and P-NC on the jute fibers exhibited the highest antimicrobial properties with the inhibition zone diameter of 18 mm whereas pristine jute shows no activity against bacteria. Furthermore, nanocellulose was also explored with viscose yarn to improve the antimicrobial properties as well. The suspension was sprayed evenly onto viscose fibre. Kokol *et al.* functionalized CNF with hexamethylenediamine (HMDA) and spray coated it onto viscose for excellent antimicrobial properties with minimal skin irritation (Fig. 10B).<sup>141</sup>

While CNF or CNC coating has been thoroughly researched for cotton fabric, there is limited literature discussing nanocellulose coating on fabrics with different compositions or characteristics. When CNF is present in low concentrations (<1%, w/w), the viscosity of the hydrogel becomes insufficient, resulting in diffusion across the fiber surface. Thus, suspen-



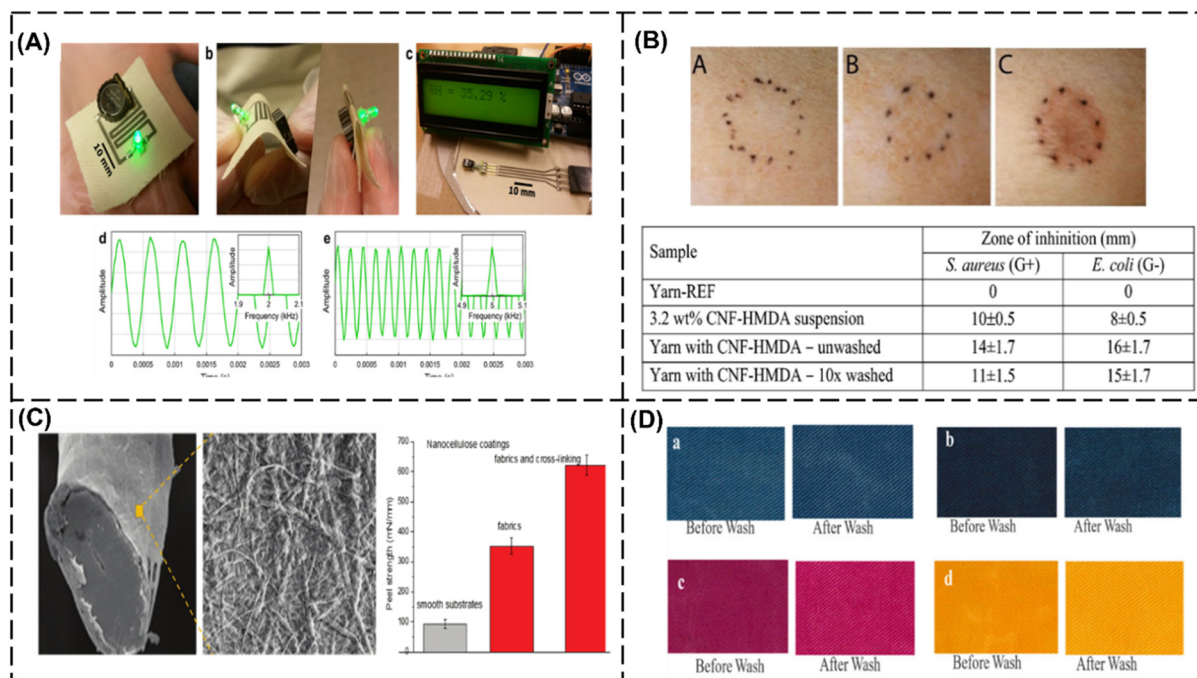


**Fig. 10** (A) a–e, the images of CNF on cotton fabrics for better inkjet printing for conductive properties. This image is adapted from © 2017 American Chemical Society.<sup>139</sup> (B) The skin irritation test on rabbit skin of (A) (3 wt%) CNF-HMD, (B) negative control and (C) positive control and the zone of inhibition of the viscose yarn and the treated viscose yarn. The images were taken from © 2021 Springer Nature.<sup>141</sup> (C) The SEM images of the nanocellulose coating and its peel strength for adhesion onto textiles, adapted from © 2020 Molecules.<sup>142</sup> (D) Images of 100% cotton woven fabric before and after five accelerated laundry cycle washing coloured with NFC dyes (a) blue, (b) black, (c) red, and (d) yellow. The image was adapted from © 2022 American Chemical Society.<sup>107</sup>

sions with high viscosity are required to achieve a substantial and uniform nanocellulose coating layer, enabling the expression of all the film-forming properties. Additionally, ozone plasma treatment can enhance the adhesion of nanocellulose to synthetic fibers by promoting the formation of hydrogen linkages with the fibers.<sup>143</sup> Saremi *et al.* performed an extensive investigation into the adhesion and water swelling resistance of CNF and CNC thin film coatings applied onto cellulose/cellophane (CL), cotton, poly(ethylene terephthalate), and nylon 6,6 (PA6,6)<sup>142</sup> (Fig. 10C). The researchers examined different adhesion techniques to understand the main mechanisms behind stabilizing coatings. In order to improve the network of nanocellulose and the bonding with the films and textiles, they introduced a cationic polyelectrolyte called poly(ethyleneimine) (PEI) to facilitate hydrogen bonding. It was expected that strong hydrogen bonds would form between the amino groups of PEI and the hydroxyl, amide, and ester groups present in the nanocellulose and textile materials. This was compared with the effects of a copolymer of glycidyl methacrylate (GMA) and oligo(ethylene glycol) methacrylate (OEGMA) (P(GMA-OEGMA)), which enhances the hydrogen bonding network and cross-links the fibers. Additionally, a commonly used cellulose cross-linker, a polycarboxylic acid (PCA) agent, was also evaluated. Tests were conducted, both in wet and dry conditions, on nanocellulose coatings applied to polymer films. The findings revealed that nanocellulose exhibi-

ted the highest adhesion on the nylon, cellulose, and cellophane surfaces, while poly(ethylene terephthalate) surfaces showed the lowest adhesion. The stability of the coatings was improved by incorporating PEI and the reactive copolymer P(GMA-OEGMA), which facilitated the formation of a cross-linked network. The addition of P(GMA-OEGMA) led to the highest adhesion and stability of the coating. Alternatively, the coating can be strengthened by cross-linking nanocellulose with polycarboxylic acids. Overall, CNC coatings demonstrate superior adhesion to all substrates compared with CNF coatings.

Liyanapathirana *et al.* developed a nano-dye carrier technology by conjugating the dye pigments onto NCF and cotton fibres with polycarboxylic acids (PCA).<sup>107</sup> The resulting dyes exhibit good colour retention of at least 90% to laundry washing cycles for different pigments (Fig. 10D). The use of nanocellulose demonstrates potential alternatives to the existing methods used in industry, be it for dye processing or restoration efforts. By the virtue of their small size and high surface area to volume ratio, very little amounts are required for the application.

#### 4.4 Smart textiles

In the dynamic realm of smart textiles, the integration of nanocellulose holds transformative potential, particularly in the domain of flexible electronics. Nanocellulose's remarkable





combination of mechanical flexibility and biocompatibility<sup>144–146</sup> lays the foundation for embedding electronic components directly into textiles. Such applications encompass flexible electronics, such as wearable sensors and even health-monitoring garments that can track vital signs.<sup>147–150</sup>

A recent work by Gao *et al.* showed the utilisation of nanocellulose in the fabrication of flexible perovskite solar cells (PSCs), which offers a sustainable solution to the growing demand for wearable electronics.<sup>151</sup> Addressing the drawbacks of non-biodegradable polymer substrates commonly used in flexible PSCs, the development of transparent nanocellulose paper (NCP) coated with acrylic resin as a substrate presents a green and biodegradable alternative. This innovation not only enhances the overall environmental footprint of flexible electronics but also ensures easy disposability. In this work, NCP-based flexible PSCs demonstrated promising results, with a power conversion efficiency (PCE) of 4.25% and remarkable stability even after 50 instances of bending. Furthermore, this concept extends beyond PSCs, as the NCP-based substrates exhibit compatibility with other electronic systems, suggesting a broader scope for next-generation green flexible electronics.

Within the domain of flexible electronics, the integration of conductive hydrogels also presents an innovative avenue for multifunctional and adaptable materials. A recent breakthrough by Han *et al.* successfully developed a versatile electroconductive hydrogel (ECH) through the incorporation of PANI@CNF (polyaniline-cellulose nanofiber) nanocomplexes into a borax-crosslinked polyvinyl alcohol (PVA) hydrogel matrix.<sup>152</sup> This work capitalizes on the synergistic properties of PANI's conductivity and CNFs' structural templating. PANI@CNF nanocomplexes were prepared through *in situ* polymerization of anilines on CNFs, which are then uniformly dispersed into the PVA gel system, yielding PANI@CNF-PVA composite ECHs. The resulting hydrogel exhibits exceptional mechanical properties, with increased compression stress and storage moduli compared with pure PVA gel. The entanglements between PVA chains, PANI@CNF complexes, and borate ions create a stable 3D network structure. This hydrogel also showcases intriguing biocompatibility, pH sensitivity, thermo-reversibility, and rapid self-healing within 15 seconds. Remarkably, the hydrogel-based electrode demonstrates substantial conductivity and specific capacitance, as well as impressive capacitance retention even after 3000 cycles. Overall, this innovative integration of conductive nanocomplexes and a biodegradable hydrogel matrix opens up exciting possibilities for the development of flexible, self-healing, and implantable electronic devices, illustrating the potential impact of nanocellulose in the realm of smart textiles.

The advent of nanocellulose-based smart textiles also opens doors to innovative solutions like monitoring masks. By incorporating nanocellulose into mask materials, it promises an environmental solution for aerosol filtration, addressing concerns related to protection against infectious diseases and environmental impact while providing biodegradability, renewability, high surface area, and functionalization potential.<sup>153</sup>

The integration of nanocellulose marks a pivotal advancement in the domain of smart textiles, particularly in the context of monitoring masks and air filtration. The challenges posed by elevated air humidity on air purification filters are effectively mitigated through ingenious strategies. For instance, Liu *et al.* have recently pioneered the creation of super-hydrophobic filters by employing a hydrophobic modification process utilizing methyltrimethoxysilane (MTMS) and CNFs.<sup>154</sup> This innovation bolsters the filters' resistance to performance degradation induced by humidity, rendering them well-suited for deployment in high humidity environments. Remarkably, the resulting air filters exhibit exceptional filtration efficiency for particulate matter (PM), achieving levels as high as 99.75% for PM1.0 and PM2.5. Coupled with low filtration resistance and a high-quality factor, this breakthrough promises transformative implications for diverse applications ranging from indoor air purification to masks, vehicles, and industrial exhaust systems, revolutionizing the landscape of air filtration within the ambit of smart textiles.

In a similar pursuit of smart textiles to enhance monitoring masks and advance aerosol filtration efficiency, Ukkola *et al.* harnessed the potential of nanostructured and porous foams derived from crosslinked CNF, sourced sustainably through deep eutectic solvent pretreatment and mechanical grinding.<sup>155</sup> The resulting nanofoams exhibit exceptional porosity and specific surface area, translating into a remarkable filtration performance. Impressively, nanofoams with varied densities showcase filtration efficiencies exceeding 96%, with a standout performance surpassing 99.5% for particles sized between 26 to 360 nm. This technology not only underscores environmental responsibility by employing biodegradable materials for filter fabrication but also promises broader applications in indoor air purification and beyond. Through such strides, nanocellulose resonates as a catalyst in propelling the smart textiles domain forward, ushering in solutions that are both efficient and ecologically conscious.

All in all, nanocellulose-based smart textiles hold potential for innovative filtration solutions, including monitoring masks. By integrating nanocellulose into masks, it addresses disease protection and environmental concerns, while offering biodegradability, renewability, and functional versatility. Strategies like super-hydrophobic filters and nanofoams from crosslinked cellulose nanofibers showcase nanocellulose's efficiency. Challenges remain in optimizing production, scalability, and adaptability. However, nanocellulose's role in driving efficient and eco-conscious solutions in smart textiles remains promising.

Furthermore, the incorporation of nanocellulose into textile-based motion sensors brings about a paradigm shift in wearable technology. Nanocellulose's flexibility and lightweight properties<sup>156</sup> are ideally suited for creating sensors that can monitor body movements, gestures, and postures, which provides diverse real-world uses of nanocellulose-based materials in tracking humans.<sup>156</sup> For example, nanocellulose-based carbon aerogels offer a multifunctional platform for the development of human body monitoring sensors. Liu *et al.*





achieved this through the intricate interplay of hydrogen bonding, electrostatic interaction, and  $\pi$ - $\pi$  interaction, resulting in conductive carbon aerogels containing cellulose nanofibrils (CNF), carbon nanotubes (CNT), and reduced graphene oxide (RGO).<sup>157</sup> These aerogels, crafted *via* bidirectional freezing and subsequent annealing, exhibit exceptional mechanical attributes, including ultralow density and superhydrophilicity. The developed superelastic aerogels, doubling as strain sensors, display good linear sensitivity and accurate human bio-signal capture. This work showed the potential of nanocellulose-based carbon aerogels in advancing wearable electronics, electronic skin, and human motion monitoring, offering a promising pathway for the integration of sustainable materials into the evolving landscape of smart textiles.

In a similar work, nanocellulose-based carbon aerogels were also used as a solution for human body monitoring sensors. In this study, Lai *et al.* characterized the developed aerogels by their remarkable compressibility and resilience.<sup>158</sup> By harnessing CNFs, a 3D lamellar structure was crafted, enabling efficient stress distribution and resistance to damage under high compression. The resulting aerogel demonstrates shape recovery and fatigue resistance, enduring extreme com-

pression strains and cycles. Bolstered by its stable architecture and high conductivity, the aerogel exhibits rapid response and sensitivity across a wide pressure range. This work showcases the immense potential of nanocellulose-based carbon aerogels in fabricating 3D tactile sensors, capable of capturing an array of human motion signals. With their versatility, resilience, and sensitivity, these aerogels pave the way for transformative applications in pressure sensors, electromagnetic shielding, and electrochemical energy storage within the realm of smart textiles.

In sum, nanocellulose is revolutionizing textiles into dynamic, interactive platforms, merging seamlessly with flexible electronics, monitoring masks, and human motion sensors. This integration introduces unprecedented functionality and responsiveness to wearable technology. From embedding electronic components to crafting superelastic, conductive carbon aerogels, nanocellulose expands the scope of textiles. However, challenges such as scalability and adaptability remain, underscoring the need for further research. Despite limitations, the era of nanocellulose-driven smart textiles is upon us, offering a gateway to sustainable, innovative applications across various industries.

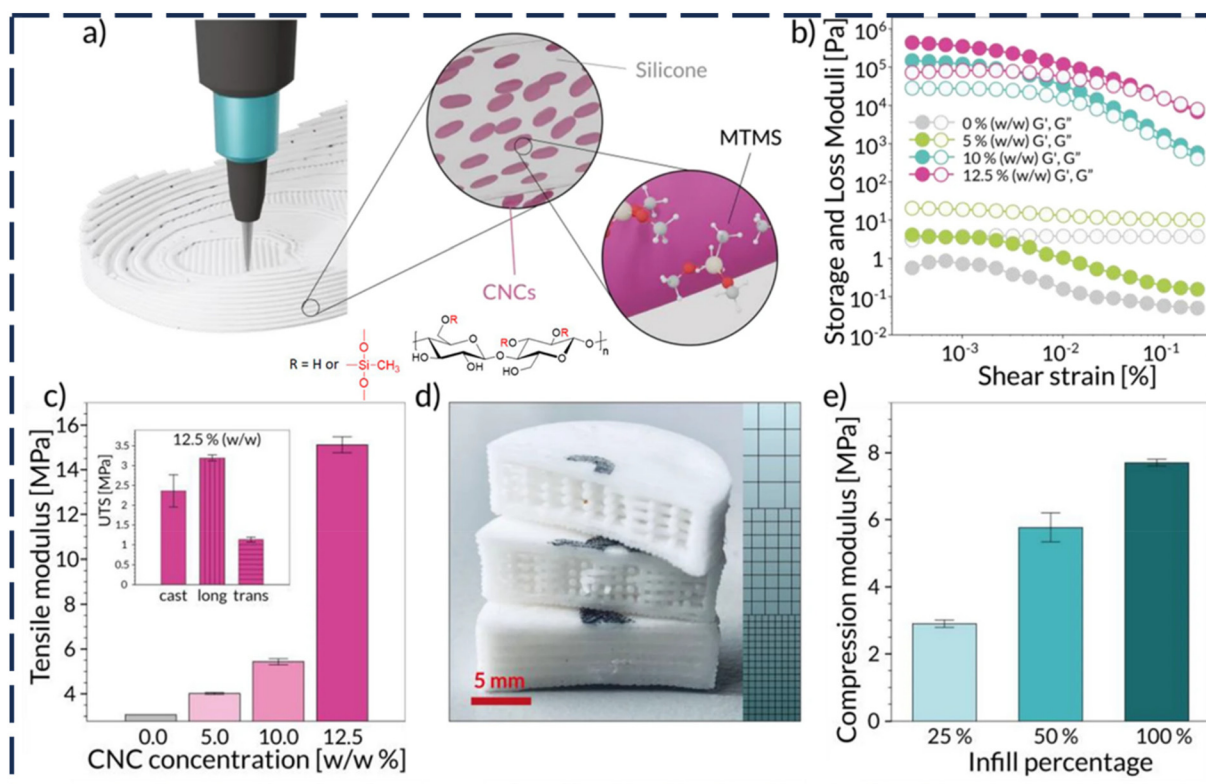


**Fig. 11** Design and characterization of structural and piezoresistive inks. (a) Schematic of the DIW printing process of the CNC-reinforced silicone resin used as structural ink. The cartoons illustrate the alignment of the surface-modified CNCs within the silicone matrix. (b) Storage and loss shear moduli of structural inks with different concentrations of CNCs. (c) Tensile moduli of composite inks prepared with distinct CNC concentrations. The inset displays the effect of the printing direction on the tensile strength of the printed parts. (d) Grid-type structures with different infill densities printed with 12.5% (w/w) CNC-reinforced ink. From bottom to top, the infill densities correspond to 100%, 50%, and 25%. (e) Compression moduli of the 12.5% CNC-reinforced ink at different infill densities. Adapted with permission from ref. 161. Copyright 2021 American Chemical Society.



#### 4.5 Renewable bio-based leather

Leather-based material is widely used in textile industry for its durability, aesthetic appeal, and a luxurious feel. Raising animals to obtain leather products can have a significant environmental impact including land use, greenhouse gas emissions, water usage, deforestation, and more.

Furthermore, leather production such as the tanning process, which preserves the leather, can also involve the use of chemicals that can be harmful to the environment if not properly managed. Also, genuine leathers are costly and require regular maintenance to keep them in good condition. Importantly, when it comes to wearable applications such as footwear and gloves, leather is heavier than many

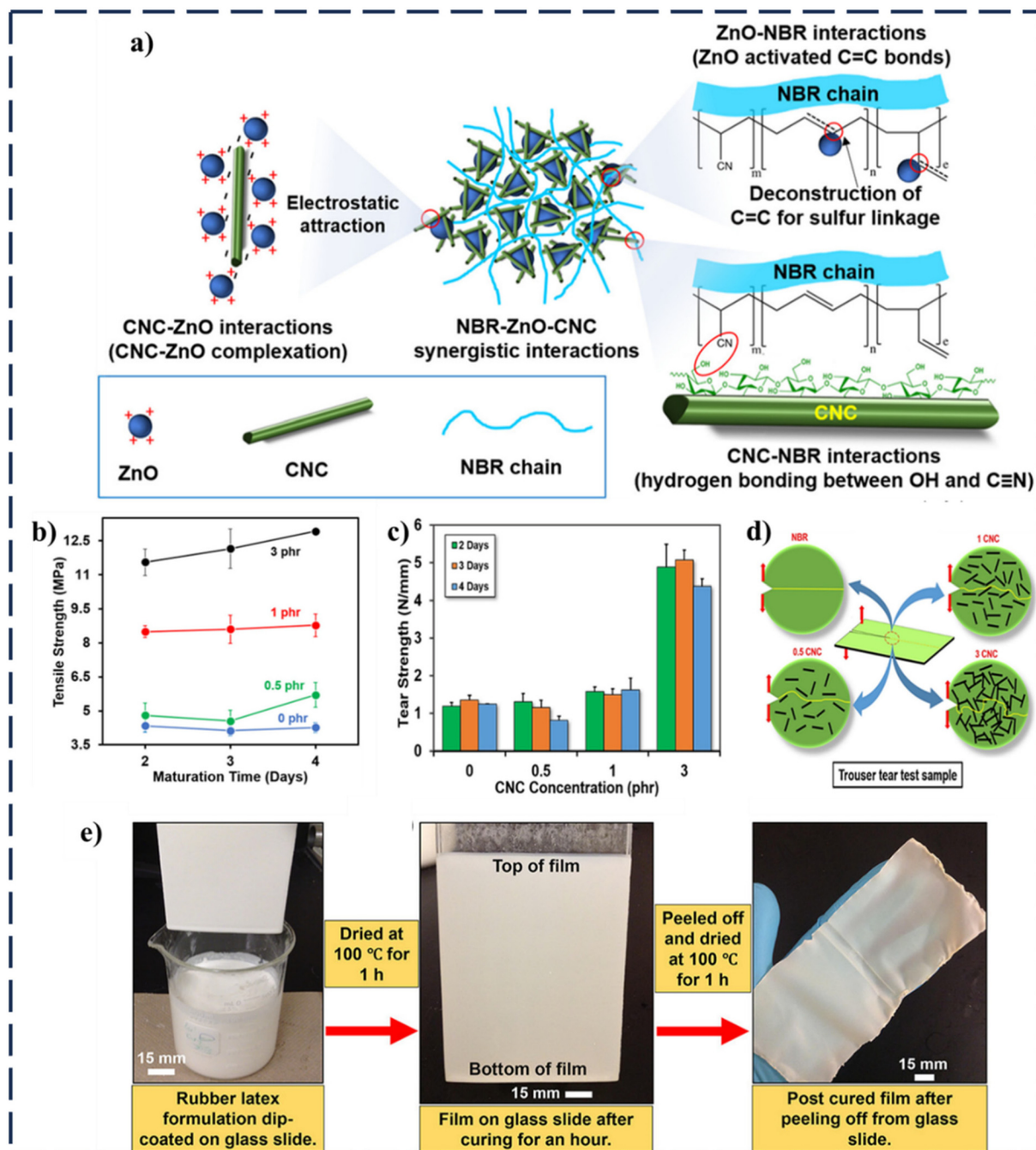


**Fig. 12** Fabrication of acrylonitrile-butadiene rubber (NBR) films with cellulose nanocrystals (CNCs) for potential gloves and other dipped goods. (a) Illustration of NBR, CNCs and ZnO synergism on the structure–property–processing of NBR films. (b) Tensile strength and (c) tear strength of NBR and NBR-nanocomposites. (d) Illustration of the percolation effect of CNC on the tear strength. Adapted with permission from ref. 162. Copyright 2021 American Chemical Society. (e) NBR-CNC film preparation by dipping method. Adapted with permission from ref. 163. Copyright 2021 American Chemical Society.



synthetic materials and can be a disadvantage in applications where weight is a critical factor.

Nanocellulose, a versatile and sustainable material which can be extracted from textile waste, is inevitably a best candidate for leather substitutes in footwear for the uppers of shoes and insoles because of its excellent mechanical strength and light weight properties. This can result in durable yet comfortable footwear. For example, nanocellulose was added in shoes manufactured by the ASICS company (Japan) in 2018 for enhanced mechanical properties.<sup>159</sup> The mechanical strength and durability of their new material reinforced by modified CNF are reported to be enhanced while keeping the light weight for application in the midsole. Nanocellulose was also added in footwear products for light weight function due to its low density property.<sup>160</sup>

In another example, silicone-based inks containing cellulose nanocrystals (CNCs) and/or carbon black fillers are used for 3D printing digital manufacturing of a fully customized smart insole with embedded piezoresistive sensors.<sup>161</sup> Functionalization of CNCs with methyltrimethoxysilane (MTMS) improves their surface compatibility with silicone, thereby aiding in the blending process with the silicone-based elastomer (Fig. 11a). Through integration of the modified CNCs into a silicone matrix, Briand *et al.* adjusted both the rheological properties of the inks and the mechanical properties of the printed material following curing (Fig. 11b). When compared with those of pure silicone, the composite comprising CNCs and silicon exhibits 2-times higher strength and 5-times higher stiffness (Fig. 11c). Apart from modifying the ink formulation, the mechanical properties of the printed components can be readily adjusted by varying the density of print lines within grid-like structures (Fig. 11d). The compressive stiffness of the grid was elevated from 3 to approximately 8 MPa by increasing the fill factor from 25 to 100% (Fig. 11e).

Besides increasing the mechanical strength of materials as a reinforcing agent, nanocellulose contains surface hydroxyl groups which allow modification and improved interactions with many materials. For instance, Mekonnen *et al.* showed the effect of CNC as a bifunctional material, crosslinking enhancer and reinforcing agent on the curing enhancement and reinforcement of acrylonitrile-butadiene rubber (NBR) latex films (Fig. 12).<sup>162</sup> CNC helped to improve the dispersion and suspension of zinc oxide (ZnO) in the latex (Fig. 12a). ZnO is an activator of the rubber chains so that sulfur can be anchored, and crosslinking initiated. Higher suspension of ZnO leads to more activated rubber sites, resulting in higher sulfur consumption during the partial interparticle crosslinking of the rubber, finally forming a higher strength material. The presence of nitrile groups on the NBR chains promotes the interactions between the CNC and the NBR chains through hydrogen bonds between the hydroxyl groups of the CNC and the nitrile moieties on the NBR chains, improving the dispersion of CNC in the NBR. With further incorporation of CNC to the NBR, the tensile strength was improved by 96 and 166% for films containing 1 and 3 phr (parts per hundred rubber) CNC, respectively, as compared

with 0 phr (Fig. 12b). For the tear strength, there were no significant changes until the CNC concentration reached 3 phr, achieving an improvement of 333% (Fig. 12c and d). In another work, they prepared dipped film samples on glass slides (Fig. 12e) and confirmed the multifold increases in tensile strengths and moduli in comparison with the base rubber matrix.<sup>163</sup>

## 5. Challenges and perspectives

This review explores the advancements in extracting, modifying, and utilizing nanocellulose from textile waste, emphasizing its critical role in various emerging applications within the textile industry. The potential for surface functionalization through hydroxyl group chemistry significantly enhances its application scope. While substantial research has focused on extracting nanocellulose from cotton-based textile waste, scaling this process to an industrial level suitable for global adoption presents considerable challenges. Intelligent classification of waste cotton using infrared spectroscopy combined with stoichiometry or multivariate statistical methods is effective but can be costly and time-consuming. Therefore, a more practical approach involves utilizing waste cotton based on demand rather than selection.

Currently, dyed waste cotton is often pretreated with bleaching, which is both environmentally harmful and expensive. Developing strategies for directly utilizing colored waste cotton is crucial. For example, extracting colored cellulose from dyed waste cotton and re-spinning it into colored rRCFs could eliminate the need for decolorization or dyeing, thereby reducing recycling costs. Future research on nanocellulose from textile waste should focus on high-value products, such as smart wearables, biomedical applications, and construction materials. Smart wearable electrode materials can be created by combining extracted nanocellulose with conductive materials like carbon nanotubes, graphene, silver nanowires, MoS<sub>2</sub>, and MXene. Advanced production technologies and processing methods, such as electrostatic spinning, wet spinning, melt spinning, 3D printing, hot pressing, freezing, and carbonization, can yield products with enhanced properties and added value. Additionally, integrating hydrophobic agents and materials with flame retardant, fluorescence, and antibacterial properties into the nanocellulose solution extracted from waste cotton can produce functional fibers or membranes through spinning or 3D printing.

The review also addresses chemical and enzymatic treatments, which are efficient in fiber separation but have economic and environmental drawbacks, impacting recycling efficiency. Mechanical fractionation can reduce fiber properties, limiting their potential for upcycling. Overcoming these challenges requires optimizing processes, reducing environmental impacts, and developing new methods for producing high-quality nanocellulose from textile waste. Investing in advanced recycling technologies that can recover fibers, including nanocellulose, from end-of-life textiles can help close the loop in textile production and reduce the need for





virgin resources. Several initiatives and projects have focused on separating cotton textile waste to address scalability and cost challenges in achieving circularity. Noteworthy projects include Tyton's, which regenerates cellulose from cotton textiles and converts PET into TPA and EG using subcritical water to break down textile waste. The resulting cellulose pulp can be processed into new textiles or nanocellulose. The "Green Machine" technology by Isko®, developed in collaboration with HKRITA and the H&M Foundation, uses ultra-efficient hydrothermal treatment to break down cotton into cellulose powders or potential nanocellulose and separate polyester from blended waste textiles, focusing on minimizing resource usage and environmental impact.<sup>164</sup> These initiatives inspire further research towards achieving a closed-loop system and expanding sustainable practices within the textile recycling sector, potentially leading to the production of nanocellulose for various applications in the textile industry.

## Data availability

No primary research results, software or code have been included and no new data were generated or analysed as part of this review.

## Conflicts of interest

There are no conflicts to declare.

## Acknowledgements

This research is supported by the RIE2025 MTC Individual Research Grants (M22K2c0085) and Central Research Fund, administered by the Agency of Science, Technology and Research (A\*STAR). This work is also supported by the National Medical Research Council (NMRC), Singapore, under its Clinician Scientist-Individual Research Grant (CS-IRG) [MOH-001357-00].

## References

- 1 R. Bick, E. Halsey and C. C. Ekenga, *Environ. Health*, 2018, **17**, 1–4.
- 2 B. Ütebay, P. Çelik and A. Çay, *Waste in textile and leather sectors*, Textile wastes: Status and perspectives, in: IntechOpen, London, 2020, ch. 3.
- 3 K. Niinimäki, G. Peters, H. Dahlbo, P. Perry, T. Rissanen and A. Gwilt, *Nat. Rev. Earth Environ.*, 2020, **1**, 189–200.
- 4 S. Liang, H. Chen, X. Zeng, Z. Li, W. Yu, K. Xiao, J. Hu, H. Hou, B. Liu and S. Tao, *Water Res.*, 2019, **159**, 242–251.
- 5 M. Todor, C. Bulei, I. Kiss and V. Alexa, *Acta Tech Corvin., Bull. Eng.*, 2019, **12**(2), 105–108.
- 6 K. Subramanian, S. S. Chopra, E. Cakin, X. Li and C. S. K. Lin, *Resour., Conserv. Recycl.*, 2020, **161**, 104989.
- 7 L. Solhi, V. Guccini, K. Heise, I. Solala, E. Niinivaara, W. Xu, K. Mihhels, M. Kröger, Z. Meng and J. Wohler, *Chem. Rev.*, 2023, **123**, 1925–2015.
- 8 Y. Jiang, X. Wang, Z. Meng, M. Zhang, S. Wang and X. Liu, *Green Chem.*, 2024, **26**, 879–894.
- 9 M. Ghasemlou, F. Daver, E. P. Ivanova, Y. Habibi and B. Adhikari, *Prog. Polym. Sci.*, 2021, **119**, 101418.
- 10 K. Dhali, M. Ghasemlou, F. Daver, P. Cass and B. Adhikari, *Sci. Total Environ.*, 2021, **775**, 145871.
- 11 E. J. Foster, R. J. Moon, U. P. Agarwal, M. J. Bortner, J. Bras, S. Camarero-Espinosa, K. J. Chan, M. J. Clift, E. D. Cranston and S. J. Eichhorn, *Chem. Soc. Rev.*, 2018, **47**, 2609–2679.
- 12 T. E. Organization, Preferred fiber and materials market report, [https://textileexchange.org/app/uploads/2022/10/Textile-Exchange\\_PFMR\\_2022.pdf](https://textileexchange.org/app/uploads/2022/10/Textile-Exchange_PFMR_2022.pdf).
- 13 R. M. Frazier, M. Lendewig, R. E. Vera, K. A. Vivas, N. Forfora, I. Azuaje, A. Reynolds, R. Venditti, J. J. Pawlak, E. Ford and R. Gonzalez, *J. Bioresour. Bioprod.*, 2024, DOI: [10.1016/j.jobab.2024.07.002](https://doi.org/10.1016/j.jobab.2024.07.002).
- 14 T. Shaikh, S. Chaudhari and A. Varma, *Int. J. Eng. Res. Ind. Appl.*, 2012, **2**, 675–680.
- 15 J. Chen, in *Textiles and fashion*, Elsevier, 2015, pp. 79–95.
- 16 S. Rana, S. Pichandi, S. Parveen and R. Fanguero, *Roadmap to sustainable textiles and clothing: environmental and social aspects of textiles and clothing supply chain*, 2014, pp. 83–123.
- 17 L. W. McKeen, in *Permeability Properties of Plastics and Elastomers*, ed. L. W. McKeen, William Andrew Publishing, 4th Edn, 2017, pp. 305–323, DOI: [10.1016/B978-0-323-50859-9.00013-0](https://doi.org/10.1016/B978-0-323-50859-9.00013-0).
- 18 B. Rodgers and W. Waddell, in *The Science and Technology of Rubber*, ed. J. E. Mark, B. Erman and C. M. Roland, Academic Press, Boston, 4th edn, 2013, pp. 653–695, DOI: [10.1016/B978-0-12-394584-6.00014-5](https://doi.org/10.1016/B978-0-12-394584-6.00014-5).
- 19 A. Pinkert, K. N. Marsh and S. Pang, *Ind. Eng. Chem. Res.*, 2010, **49**, 11121–11130.
- 20 A. J. Sayyed, N. A. Deshmukh and D. V. Pinjari, *Cellulose*, 2019, **26**, 2913–2940.
- 21 C. Olsson and G. Westman, *Cellul.: Fundam. Aspects*, 2013, **10**, 52144.
- 22 K. J. Edgar and H. Zhang, *Carbohydr. Polym.*, 2020, **250**, 116932.
- 23 M. N. Alam and L. P. Christopher, *Carbohydr. Polym.*, 2017, **173**, 253–258.
- 24 Y. Ertas and T. Uyar, *Carbohydr. Polym.*, 2017, **177**, 378–387.
- 25 Y. Watabe, Y. Suzuki, S. Koike, S. Shimamoto and Y. Kobayashi, *J. Dairy Sci.*, 2018, **101**, 10929–10938.
- 26 K. Kamide and K. Nishiyama, *Regenerated Cellulose Fibers*, 2001, pp. 88–155.
- 27 S. Bi, L. Hou, H. Zhao, L. Zhu and Y. Lu, *J. Mater. Chem. A*, 2018, **6**, 16556–16565.
- 28 M. Sampath, S. Mani and G. Nalankilli, *J. Ind. Text.*, 2011, **41**, 160–173.
- 29 J. A. Foulk and D. D. Mcalister III, *Text. Res. J.*, 2002, **72**, 885–891.





- 30 W. Wardiningsih, *Study of comfort properties of natural and synthetic knitted fabrics in different blend ratios for winter active sportswear*, A thesis submitted in the degree of Master of Technology, School of Fashion and Textiles Design and Social Context RMIT University, Melbourne June, 2009.
- 31 R. Chollakup, A. Sinoimeri, J.-F. Osselin, R. Frydrych and J.-Y. Dréan, *Res. J. Text. Apparel*, 2005, **9**, 57–69.
- 32 N. Pensupa, in *Sustainable Technologies for Fashion and Textiles*, Elsevier, 2020, pp. 251–309.
- 33 A. P. Kumar, D. Depan, N. S. Tomer and R. P. Singh, *Prog. Polym. Sci.*, 2009, **34**, 479–515.
- 34 A. Tribot, G. Amer, M. A. Alio, H. de Baynast, C. Delattre, A. Pons, J.-D. Mathias, J.-M. Callois, C. Vial and P. Michaud, *Eur. Polym. J.*, 2019, **112**, 228–240.
- 35 X. Luo and X. Wang, *BioResources*, 2017, **12**, 5826–5837.
- 36 J. A. Pérez, A. Gonzalez, J. M. Oliva, I. Ballesteros and P. Manzanares, *J. Chem. Technol. Biotechnol.*, 2007, **82**, 929–938.
- 37 E. Espinosa, I. Bascón-Villegas, A. Rosal, F. Pérez-Rodríguez, G. Chinga-Carrasco and A. Rodríguez, *Int. J. Biol. Macromol.*, 2019, **141**, 197–206.
- 38 Z. Wang, Z. Yao, J. Zhou and Y. Zhang, *Carbohydr. Polym.*, 2017, **157**, 945–952.
- 39 M. Le Troedec, D. Sedan, C. Peyratout, J. P. Bonnet, A. Smith, R. Guinebreiere, V. Gloaguen and P. Krausz, *Composites, Part A*, 2008, **39**, 514–522.
- 40 D. Damayanti, L. A. Wulandari, A. Bagaskoro, A. Rianjanu and H.-S. Wu, *Polymers*, 2021, **13**, 3834.
- 41 S. Björquist, Dissertation on Separation for regeneration: Chemical recycling of cotton and polyester textiles, 2017, <https://publications.lib.chalmers.se/records/fulltext/249870/249870.pdf>.
- 42 J. Aronsson and A. Persson, *J. Eng. Fibers Fabr.*, 2020, **15**, 1558925020901322.
- 43 G. Chroona, Dissertation on Fractionation of textile fibres from denim jeans, 2016, <https://www.diva-portal.org/smash/get/diva2:1109624/FULLTEXT01.pdf>.
- 44 A. Ouchi, T. Toida, S. Kumaresan, W. Ando and J. Kato, *Cellulose*, 2010, **17**, 215–222.
- 45 S. Sakthivel, B. Melese, A. Edae, F. Abedom, S. Mekonnen and E. Solomon, *Adv. Mater. Sci. Eng.*, 2020, **2020**, 1–8.
- 46 S. Jiang, Z. Xia, A. Farooq, M. Zhang, M. Li and L. Liu, *Cellulose*, 2021, **28**, 3235–3248.
- 47 X. Kang, S. Kuga, C. Wang, Y. Zhao, M. Wu and Y. Huang, *ACS Sustainable Chem. Eng.*, 2018, **6**, 2954–2960.
- 48 J. S. Kim, Y. Lee and R. W. Torget, *Twenty-Second Symposium on Biotechnology for Fuels and Chemicals*, Humana Press, 2001, 331–340.
- 49 A. B. Perumal, R. B. Nambiar, J. Moses and C. Anandharamakrishnan, *Food Hydrocolloids*, 2022, **127**, 107484.
- 50 T. Zhong, R. Dhandapani, D. Liang, J. Wang, M. P. Wolcott, D. Van Fossen and H. Liu, *Carbohydr. Polym.*, 2020, **240**, 116283.
- 51 N. Pandi, S. H. Sonawane and K. A. Kishore, *Ultrason. Sonochem.*, 2021, **70**, 105353.
- 52 J. Cao, X. Sun, C. Lu, Z. Zhou, X. Zhang and G. Yuan, *Carbohydr. Polym.*, 2016, **149**, 60–67.
- 53 J. P. S. Morais, M. de Freitas Rosa, L. D. Nascimento, D. M. Do Nascimento and A. R. Cassales, *Carbohydr. Polym.*, 2013, **91**, 229–235.
- 54 S. Thambiraj and D. R. Shankaran, *Appl. Surf. Sci.*, 2017, **412**, 405–416.
- 55 P.-Y. Kuo, N. Yan and M. Sain, *Eur. Polym. J.*, 2013, **49**, 3778–3787.
- 56 A. K. Rana, E. Frollini and V. K. Thakur, *Int. J. Biol. Macromol.*, 2021, **182**, 1554–1581.
- 57 D. Pradhan, A. K. Jaiswal and S. Jaiswal, *Carbohydr. Polym.*, 2022, **285**, 119258.
- 58 S. Ye, H.-Y. Yu, D. Wang, J. Zhu and J. Gu, *Cellulose*, 2018, **25**, 5139–5155.
- 59 N. T. U. Culsum, C. Melinda, I. Leman, A. Wibowo and Y. W. Budhi, *Mater. Today Commun.*, 2021, **26**, 101817.
- 60 L. Feng and Z.-l. Chen, *J. Mol. Liq.*, 2008, **142**, 1–5.
- 61 A. Poulouse, J. Parameswaranpillai, J. J. George, J. A. Gopi, S. Krishnasamy, M. Dominic CD, N. Hameed, N. V. Salim, S. Radoor and N. Sienkiewicz, *Molecules*, 2022, **27**, 8032.
- 62 A. H. Bhat, I. Khan, M. A. Usmani, R. Umapathi and S. M. Z. Al-Kindy, *Int. J. Biol. Macromol.*, 2019, **129**, 750–777.
- 63 G. Meister and M. Wechsler, *Biodegradation*, 1998, **9**, 91–102.
- 64 A. Jeihanipour, K. Karimi, C. Niklasson and M. J. Taherzadeh, *Waste Manage.*, 2010, **30**, 2504–2509.
- 65 L. V. Haule, C. Carr and M. Rigout, *J. Cleaner Prod.*, 2016, **112**, 4445–4451.
- 66 F. Lv, C. Wang, P. Zhu and C. Zhang, *Carbohydr. Polym.*, 2015, **123**, 424–431.
- 67 T.-M. Tenhunen, A. E. Lewandowska, H. Orelma, L.-S. Johansson, T. Virtanen, A. Harlin, M. Österberg, S. J. Eichhorn and T. Tammelin, *Cellulose*, 2018, **25**, 137–150.
- 68 Y.-L. Chen, X. Zhang, T.-T. You and F. Xu, *Cellulose*, 2019, **26**, 205–213.
- 69 O. Azougagh, S. Essayeh, N. Achalhi, A. El Idrissi, H. Amhamdi, M. Loutou, Y. El Ouardi, A. Salhi, M. Abou-Salama and S. El Barkany, *Carbohydr. Polym.*, 2022, **276**, 118737.
- 70 P. Willberg-Keyriläinen, J. Hiltunen and J. Ropponen, *Cellulose*, 2018, **25**, 195–204.
- 71 Z. Ling, J. Edwards, G. Zongwei, N. Prevost, S. Nam, Q. Wu, A. French and F. Xu, *Cellulose*, 2019, **26**, 861–876.
- 72 L. Liu, H. Yao, Q. Zhou, X. Yao, D. Yan, J. Xu and X. Lu, *J. Environ. Chem. Eng.*, 2022, **10**, 107512.
- 73 M. Wang, S. Shi, F. Li, W. Hou, H. Guo, W. Shuhua, H. Jia and J. Dai, *Chem. Pap.*, 2022, **76**, 1–12.
- 74 Z. Wang, Z. Yao, J. Zhou, M. He, Q. Jiang, A. Li, S. Li, M. Liu, S. Luo and D. Zhang, *Int. J. Biol. Macromol.*, 2019, **129**, 878–886.
- 75 M. M. Á. D. Maciel, K. C. C. de Carvalho Benini, H. J. C. Voorwald and M. O. H. Cioffi, *Int. J. Biol. Macromol.*, 2019, **126**, 496–506.



- 76 F. Hemmati, S. M. Jafari and R. A. Taheri, *Int. J. Biol. Macromol.*, 2019, **137**, 374–381.
- 77 J. H. Jordan, M. W. Easson, B. Dien, S. Thompson and B. D. Condon, *Cellulose*, 2019, **26**, 5959–5979.
- 78 Y. Sun, Z. Xia, A. Yang, J. Li, L. Wang, H. Chen, X. Zheng and Y. Liu, *J. Phys. Conf. Ser.*, 2021, **1790**(1), 12074, IOP Publishing.
- 79 A. B. Vanzetto, L. V. R. Beltrami and A. J. Zattera, *Cellulose*, 2021, **28**, 6967–6981.
- 80 S. Rizal, F. Olaiya, N. Saharudin, C. Abdullah, N. G. Olaiya, M. M. Haafiz, E. Yahya and F. Sabaruddin, *Polymers*, 2021, **13**, 325.
- 81 P. K. Mishra, A. Ahuja, B. K. Mahur and V. K. Rastogi, *EXPRESS Polym. Lett.*, 2023, **17**, 196–210.
- 82 P. Srichola, K. Witthayolankowit, P. Sukyai, C. Sampoompuang, K. Lobyam, P. Kampakun and R. Toomtong, *Polymers*, 2023, **15**, 3324.
- 83 R. P. Mari, J. J. Sornas and A. C. Bierhalz, *Cellulose*, 2023, **30**, 1657–1668.
- 84 X.-Q. Chen, G.-X. Pang, W.-H. Shen, X. Tong and M.-Y. Jia, *Carbohydr. Polym.*, 2019, **207**, 713–719.
- 85 N. G. Olaiya, A. A. Oyekanmi, M. M. Hanafiah, T. O. Olugbade, M. K. Adeyeri and F. G. Olaiya, *Bioresour. Technol. Rep.*, 2022, **19**, 101183.
- 86 M. B. Noremylia, M. Z. Hassan and Z. Ismail, *Int. J. Biol. Macromol.*, 2022, **206**, 954–976.
- 87 E. Gholamzad, K. Karimi and M. Masoomi, *Chem. Eng. J.*, 2014, **253**, 40–45.
- 88 M.-X. Ruiz-Caldas, J. Carlsson, I. Sadiktsis, A. Jaworski, U. Nilsson and A. P. Mathew, *ACS Sustainable Chem. Eng.*, 2022, **10**, 3787–3798.
- 89 Y. Li, J. Peng, X. Liu, D. Song, W. Xu and K. Zhu, *Polymer*, 2021, **237**, 124349.
- 90 T. A. Khattab, M. S. Abdelrahman and M. Rehan, *Environ. Sci. Pollut. Res.*, 2020, **27**, 3803–3818.
- 91 B. Lellis, C. Z. Fávaro-Polonio, J. A. Pamphile and J. C. Polonio, *Biotechnol. Res. Innov.*, 2019, **3**, 275–290.
- 92 A. Aldalbahi, M. E. El-Naggar, M. H. El-Newehy, M. Rahaman, M. R. Hatshan and T. A. Khattab, *Polymers*, 2021, **13**, 155.
- 93 R. Al-Tohamy, S. S. Ali, F. Li, K. M. Okasha, Y. A. G. Mahmoud, T. Elsamahy, H. Jiao, Y. Fu and J. Sun, *Ecotoxicol. Environ. Saf.*, 2022, **231**, 113160.
- 94 D. A. Yaseen and M. Scholz, *Int. J. Environ. Sci. Technol.*, 2019, **16**, 1193–1226.
- 95 K. Piaskowski, R. Świdarska-Dąbrowska and P. K. Zarzycki, *J. AOAC Int.*, 2018, **101**, 1371–1384.
- 96 S. Dutta, B. Gupta, S. K. Srivastava and A. K. Gupta, *Mater. Adv.*, 2021, **2**, 4497–4531.
- 97 A. Qiao, M. Cui, R. Huang, G. Ding, W. Qi, Z. He, J. J. Klemeš and R. Su, *Carbohydr. Polym.*, 2021, **272**, 118471.
- 98 M. Tavakolian, H. Wiebe, M. A. Sadeghi and T. G. M. van de Ven, *ACS Appl. Mater. Interfaces*, 2020, **12**, 5040–5049.
- 99 M. Bassyouni, M. S. Zoromba, M. H. Abdel-Aziz and I. Mosly, *Polymers*, 2022, **14**, 1852.
- 100 J. Tang, Y. Song, F. Zhao, S. Spinney, J. da Silva Bernardes and K. C. Tam, *Carbohydr. Polym.*, 2019, **208**, 404–412.
- 101 N. Amiralian, M. Mustapic, M. S. A. Hossain, C. Wang, M. Konarova, J. Tang, J. Na, A. Khan and A. Rowan, *J. Hazard. Mater.*, 2020, **394**, 122571.
- 102 S. Velusamy, A. Roy, S. Sundaram and T. Kumar Mallick, *Chem. Rec.*, 2021, **21**, 1570–1610.
- 103 R. Sujanani, M. R. Landsman, S. Jiao, J. D. Moon, M. S. Shell, D. F. Lawler, L. E. Katz and B. D. Freeman, *ACS Macro Lett.*, 2020, **9**, 1709–1717.
- 104 P. Liu, P. F. Borrell, M. Božič, V. Kokol, K. Oksman and A. P. Mathew, *J. Hazard. Mater.*, 2015, **294**, 177–185.
- 105 M. Li, S. A. Messele, Y. Boluk and M. Gamal El-Din, *Carbohydr. Polym.*, 2019, **221**, 231–241.
- 106 L. Spagnuolo, R. D'Orsi and A. Operamolla, *ChemPlusChem*, 2022, **87**, e202200204.
- 107 A. Liyanapathirana, M. J. Peña, S. Sharma and S. Minko, *ACS Omega*, 2020, **5**, 9196–9203.
- 108 A. Salama, R. Abouzeid, W. S. Leong, J. Jeevanandam, P. Samyn, A. Dufresne, M. Bechelany and A. Barhoum, *Nanomaterials*, 2021, **11**, 3008.
- 109 D. Chattopadhyay and B. Patel, *J. Text. Sci. Eng.*, 2016, **6**, 2.
- 110 S. Rai, R. Saremi, S. Sharma and S. Minko, *Green Chem.*, 2021, **23**, 7937–7944.
- 111 T. Lohtander, N. Durandin, T. Laaksonen, S. Arola and P. Laaksonen, *J. Cleaner Prod.*, 2021, **328**, 129615.
- 112 R. Hendrickx, G. Desmarais, M. Weder, E. S. Ferreira and D. Derome, *J. Cult. Herit.*, 2016, **19**, 445–453.
- 113 K. Kolman, O. Nechyporchuk, M. Persson, K. Holmberg and R. Bordes, *Colloids Surf., A*, 2017, **532**, 420–427.
- 114 B. W. Keyser, *J. Am. Inst. Conserv.*, 1984, **24**, 1–13.
- 115 O. Nechyporchuk, K. Kolman, A. Bridarolli, M. Odlyha, L. Bozec, M. Oriola, G. Campo-Francés, M. Persson, K. Holmberg and R. Bordes, *Carbohydr. Polym.*, 2018, **194**, 161–169.
- 116 A. Bridarolli, M. Odlyha, O. Nechyporchuk, K. Holmberg, C. Ruiz-Recasens, R. Bordes and L. Bozec, *ACS Appl. Mater. Interfaces*, 2018, **10**, 33652–33661.
- 117 J. Wang, B. Yiu, J. Obermeyer, C. D. Filipe, J. D. Brennan and R. Pelton, *Biomacromolecules*, 2012, **13**, 559–564.
- 118 K. Kolman, O. Nechyporchuk, M. Persson, K. Holmberg and R. Bordes, *ACS Appl. Nano Mater.*, 2018, **1**, 2036–2040.
- 119 D. Chelazzi, A. Chevalier, G. Pizzorusso, R. Giorgi, M. Menu and P. Baglioni, *Polym. Degrad. Stab.*, 2014, **107**, 314–320.
- 120 O. Chiantore and M. Lazzari, *Polymer*, 2001, **42**, 17–27.
- 121 C. Cianci, D. Chelazzi, G. Poggi, F. Modi, R. Giorgi and M. Laurati, *Colloids Surf., A*, 2022, **634**, 127944.
- 122 D. Chattopadhyay and B. Patel, *J. Text. Sci. Eng.*, 2016, **06**, 2.
- 123 Q.-Y. Cheng, C.-S. Guan, M. Wang, Y.-D. Li and J.-B. Zeng, *Carbohydr. Polym.*, 2018, **199**, 390–396.
- 124 M. Zaman, H. Liu, H. Xiao, F. Chibante and Y. Ni, *Carbohydr. Polym.*, 2013, **91**, 560–567.
- 125 D. Neto and P. B. Silva, *Biomed. J. Sci. Tech. Res.*, 2020, **27**, 20402–20409.



- 126 H. Xiang, B. Wang, M. Zhong, W. Liu, D. Yu, Y. Wang, K. C. Tam, G. Zhou and Z. Zhang, *ACS Sustainable Chem. Eng.*, 2022, **10**, 5939–5948.
- 127 L. Lu, S. Fan, Q. Niu, Q. Peng, L. Geng, G. Yang, H. Shao, B. S. Hsiao and Y. Zhang, *ACS Sustainable Chem. Eng.*, 2019, **7**, 14765–14774.
- 128 B. Mortimer, J. Guan, C. Holland, D. Porter and F. Vollrath, *Acta Biomater.*, 2015, **11**, 247–255.
- 129 X. Yang, Z. Wang, Y. Zhang and W. Liu, *Fibers Polym.*, 2020, **21**, 2521–2529.
- 130 M. Li, A. Farooq, S. Jiang, M. Zhang, H. Mussana and L. Liu, *Text. Res. J.*, 2021, **91**, 2303–2314.
- 131 D. Gupta and M. Gulrajani, *Functional Finishes for Textiles*, Woodhead Publishing, 2015, vol. 2014, pp. 257–281.
- 132 X. Jiang, X. Tian, J. Gu, D. Huang and Y. Yang, *Appl. Surf. Sci.*, 2011, **257**, 8451–8456.
- 133 G. Doganli, B. Yuzer, I. Aydin, T. Gultekin, A. H. Con, H. Selcuk and S. Palamutcu, *J. Coat. Technol. Res.*, 2016, **13**, 257–265.
- 134 B. M. Kale, J. Wiener, J. Militky, S. Rwawiire, R. Mishra, K. I. Jacob and Y. Wang, *Carbohydr. Polym.*, 2016, **150**, 107–113.
- 135 S. M. Saleh, T. Hassan, H. Idrees, T. M. Zaghlol and M. A. Badr, *Egypt. J. Chem.*, 2023, **66**, 187–196.
- 136 X. Yang, Z. Wang, Y. Zhang and W. Liu, *Fibers Polym.*, 2020, **21**, 2521–2529.
- 137 A. Jebali, S. Hekmatimoghaddam, A. Behzadi, I. Rezapour, B. H. Mohammadi, T. Jasemizad, S. A. Yasini, M. Javadzadeh, A. Amiri, M. Soltani, Z. Rezaei, N. Sedighi, M. Seyfi, M. Rezaei and M. Sayadi, *Cellulose*, 2013, **20**, 2897–2907.
- 138 D. R. Alvarado, D. S. Argyropoulos, F. Scholle, B. S. T. Peddinti and R. A. Ghiladi, *Green Chem.*, 2019, **21**, 3424–3435.
- 139 O. Nechyporchuk, J. Yu, V. A. Nierstrasz and R. Bordes, *ACS Sustainable Chem. Eng.*, 2017, **5**, 4793–4801.
- 140 A. M. El-Shafei, A. M. Adel, A. A. Ibrahim and M. T. Al-Shemy, *Int. J. Biol. Macromol.*, 2019, **124**, 733–741.
- 141 V. Kokol, V. Vivod, Z. Peršin, M. Čolić and M. Kolar, *Cellulose*, 2021, **28**, 6545–6565.
- 142 R. Saremi, N. Borodinov, A. M. Laradji, S. Sharma, I. Luzinov and S. Minko, *Molecules*, 2020, **25**, 3238.
- 143 J. d'Eon, W. Zhang, L. Chen, R. M. Berry and B. Zhao, *Cellulose*, 2017, **24**, 1877–1888.
- 144 Z. Chen, Y. Hu, G. Shi, H. Zhuo, M. A. Ali, E. Jamróz, H. Zhang, L. Zhong and X. Peng, *Adv. Funct. Mater.*, 2023, **33**, 2214245.
- 145 M. Y. Khalid, A. Al Rashid, Z. U. Arif, W. Ahmed and H. Arshad, *J. Mater. Res. Technol.*, 2021, **14**, 2601–2623.
- 146 M. N. Norizan, S. S. Shazleen, A. H. Alias, F. A. Sabaruddin, M. R. M. Asyraf, E. S. Zainudin, N. Abdullah, M. S. Samsudin, S. H. Kamarudin and M. N. F. Norrrahim, *Nanomaterials*, 2022, **12**, 3483.
- 147 A. Horta-Velázquez and E. Morales-Narváez, *Green Anal. Chem.*, 2022, **1**, 100009.
- 148 M. M. Langari, M. Nikzad and J. Labidi, *Carbohydr. Polym.*, 2023, **304**, 120509.
- 149 G. Dandegaonkar, A. Ahmed, L. Sun, B. Adak and S. Mukhopadhyay, *Mater. Adv.*, 2022, **3**, 3766–3783.
- 150 M. Popescu and C. Ungureanu, *Journal*, 2023, **16**, 486.
- 151 L. Gao, L. Chao, M. Hou, J. Liang, Y. Chen, H.-D. Yu and W. Huang, *npj Flexible Electron.*, 2019, **3**, 4.
- 152 J. Han, Q. Ding, C. Mei, Q. Wu, Y. Yue and X. Xu, *Electrochim. Acta*, 2019, **318**, 660–672.
- 153 T. T. Stanislas, K. Bilba, R. P. de Oliveira Santos, C. Onésippe-Potiron, H. Savastano Junior and M. A. Arsène, *Cellulose*, 2022, **29**, 8001–8024.
- 154 T. Liu, C. Cai, R. Ma, Y. Deng, L. Tu, Y. Fan and D. Lu, *ACS Appl. Mater. Interfaces*, 2021, **13**, 24032–24041.
- 155 J. Ukkola, M. Lampimäki, O. Laitinen, T. Vainio, J. Kangasluoma, E. Siivola, T. Petäjä and H. Liimatainen, *J. Cleaner Prod.*, 2021, **310**, 127498.
- 156 F. Ji, Z. Sun, T. Hang, J. Zheng, X. Li, G. Duan, C. Zhang and Y. Chen, *Compos. Commun.*, 2022, **35**, 101351.
- 157 H. Liu, T. Xu, C. Cai, K. Liu, W. Liu, M. Zhang, H. Du, C. Si and K. Zhang, *Adv. Funct. Mater.*, 2022, **32**, 2113082.
- 158 H. Lai, H. Zhuo, Y. Hu, G. Shi, Z. Chen, L. Zhong and M. Zhang, *ACS Sustainable Chem. Eng.*, 2021, **9**, 9761–9769.
- 159 B. Wu, S. Wang, J. Tang and N. Lin, in *Advanced Functional Materials from Nanopolysaccharides*, ed. N. Lin, J. Tang, A. Dufresne and M. K. C. Tam, Springer Singapore, Singapore, 2019, pp. 389–409, DOI: [10.1007/978-981-15-0913-1\\_11](https://doi.org/10.1007/978-981-15-0913-1_11).
- 160 W. Hao, M. Wang, F. Zhou, H. Luo, X. Xie, F. Luo and R. Cha, *Carbohydr. Polym.*, 2020, **243**, 116466.
- 161 M. R. Binelli, R. van Dommelen, Y. Nagel, J. Kim, R. I. Haque, F. B. Coulter, G. Siqueira, A. R. Studart and D. Briand, *Sci. Rep.*, 2023, **13**, 1962.
- 162 E. Ogunsona, S. Hojabr, R. Berry and T. H. Mekonnen, *Int. J. Biol. Macromol.*, 2020, **164**, 2038–2050.
- 163 R. Blanchard, E. O. Ogunsona, S. Hojabr, R. Berry and T. H. Mekonnen, *ACS Appl. Polym. Mater.*, 2020, **2**, 887–898.
- 164 Isko, HKRITA Green Machine for Isko, Innovation in Textiles, 2021, <https://www.innovationintextiles.com/hkrita-green-machine-for-isko/>.

